

Optimization of Dielectric Substrate Properties to Design Patch Antenna for Coastal Surveillance

A thesis submitted to
University of the Petroleum and Energy Studies

For the Award of
Doctor of Philosophy
in
Electronics and Communication Engineering

by
Madhukant Patel
SAP ID: 500034429

December 2021

SUPERVISOR

Dr. (Prof.) Piyush Kuchhal
Department of Applied Sciences, UPES, Dehradun

EXTERNAL SUPERVISOR

Dr. Kanhaiya Lal
Director RF&MW, Sahajanand Laser Technology, Gandhinagar



Department of Electrical and Electronics Engineering
School of Engineering
University of the Petroleum and Energy Studies
Dehradun-248007: Uttarkhand

Optimization of Dielectric Substrate Properties to Design Patch Antenna for Coastal Surveillance

A thesis submitted to
University of the Petroleum and Energy Studies

For the Award of
Doctor of Philosophy
in
Electronics and Communication Engineering

by
Madhukant Patel

December 2021

SUPERVISORs

Dr. (Prof.) Piyush Kuchhal

Dr. Kanhaiya Lal



Department of Electrical and Electronics Engineering
School of Engineering
University of the Petroleum and Energy Studies
Dehradun-248007: Uttarkhand

DECLARATION

I declare that the thesis entitled as **Optimization of dielectric substrate properties to design Patch antenna for coastal surveillance** has been prepared by me under the guidance of Dr. Piyush Kuchhal, Professor, Applied Science, UPES, Dehradun and Dr. Kanhaiya Lal, Director, RF & Microwave Division, Sahajanand Laser Technology, Gandhinagar. No part of this thesis has formed the basis for the award of any degree or fellowship previously.



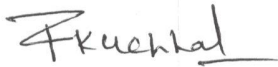
Madhukant Patel

(SAP 500034429)

Department of Electrical and Electronics Engineering,
University of Petroleum and Energy Studies,
Dehradun-248007: Uttarakhand.

CERTIFICATE

I certify that Mr. Madhukant Patel has prepared his thesis entitled “**Optimization of dielectric substrate properties to design patch antenna for coastal surveillance**”, for the award of Ph.D. degree of the University of Petroleum & Energy Studies, under my guidance. He has carried out the work at the Department of Electrical & Electronics Engineering, University of Petroleum & Energy Studies.



Dr. Piyush Kuchhal

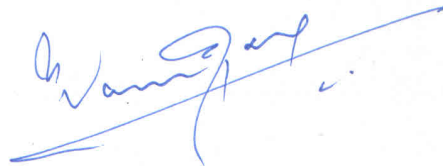
Professor,
Department of Applied Science,
University of Petroleum and Energy Studies,
Dehradun-248007: Uttarakhand.

Date: December, 2021.

CERTIFICATE

I certify that Mr. Madhukant Patel has prepared his thesis entitled “**Optimization of dielectric substrate properties to design patch antenna for coastal surveillance**”, for the award of Ph.D. degree of the University of Petroleum & Energy Studies, under my guidance. He has carried out the work at the Department of Electrical & Electronics Engineering, University of Petroleum & Energy Studies.

External Supervisor



[Dr. Kanhaiya Lal]

**Director, RF & Microwave Division,
Sahajanand Laser Technology, Associate Professor,
Gandhinagar, Gujrat.**

Date: November, 2021.

Sahajanand Laser Technology Ltd.

**ISO
9001-2015**

Regd. Office & Works - 1
E-30, G. I. D. C. Electronic Estate,
Sector-26, Gandhinagar - 382 028,
Gujarat, India.
Tel : +91-79-6170-1616
+91-79-2328-7461-63-64
Fax : 079-2328-7470

Works - 2
E-2, G.I.D.C., Electronic Estate,
Sec.-26, Gandhinagar - 382 028,
Gujarat, India.
Tel : +91-79-6170-1616
+91-79-2328-7461-63-64
Fax : 079-2328-7470

Works - 3
A-8, G.I.D.C., Electronic Estate,
Sec.-25, Gandhinagar - 382 - 016,
Gujarat, India.
Tel : +91-79-6170-1616
+91-79-2328-7461-63-64

Mumbai Office
315 - 3rd Floor, Diamoda Gold Building,
Tanvi Complex, Near Dahisar Petrol Pump,
S V Road, Dahisar (East),
Mumbai - 400 068, Maharashtra, INDIA.
Tel : +91-88-7933-6213 / 14

SEZ Works
Plot No. 233, Venus Building,
Beside J.B. Diamond,
L.H. Road, Varachha,
Surat - 395 006, Gujarat, India.
Tel : +91-261-2543440 / 2548440

Abstract

To design Microwave sensors for coastal line security was never easy in India. Being a very long and sensitive coastal line with harsh terrains in India, it demands a very high reliable and cost effective solution for this purpose. Most part of the coastal border is sensitive to smuggling activities, human intrusions, drug trafficking and veponary transportation. Detection of human intrusion in all weather such as rainy, foggy or dark nights is of utmost importance.

Based on the initial discussion with stakeholders such as ISRO, Coast guard, microwave experts, it need for high quality microwave substrate for x-band frequency, and take forward the customisation on this material so that it can become usable for sensors in microwave patch antenna arrays.

The aim of the this research work inVolves in design, fabrication and testing along with challenges inVolved in the detailed formulation of the algorithm for detecting the intrusion activities in real situation.

It was found during initial literature survey and from subject experts that the technology developed by Governments, Corporates and Researchers was not adequately scalable and affordable. It was also found that the end-to-end solution is not thought of by many researchers and Government agencies for this purpose. It was also emerging that, so far, very little efforts have been put in to design the ‘very high quality’ dielectric material for X-band in India. Practically least work has been done on high quality laminated copper cladding sheets and make them achievable in India.

Based on a gap analysis, it was also observed that not much work has been done for detection and prevention of illegal activities on coastal lines such as smuggling

and infiltration. At present, most of measures concentrate on small scale coastal line activities of the coast guard and border security forces, which are insufficient to cover the large Indian coastline. Highly dependable, reliable, scalable, cost effective and intelligent automation technologies systems are needed to secure the national borders.

To address these issues, thesis is focused on an important aspect of designing a high quality dielectric material for microwave sensors along with its evaluation against Roger RO3006, and FR4 material. The performance of the patch array designed with these two easy available material are affected by environmental uncertainties particularly in coastal line. A power efficient and highly stable dielectric material has been realised and used in patch antenna that has been evaluated against the other leading materials. To achieve the research aim highly customised, effective and affordable indigenous material is developed.

The main step of the research carried out is designing and manufacturing the material with very high dielectric coefficient. The material realised possesses property including low loss, flexible, environmentally stable, stable against mechanical stress and affordable since it uses Butyl and TiO_2 , which are available abundantly in the country. The new dielectric material has been compared and validated with FR4 and Roger RO3006, which are used by the industries globally. The dielectric constant of the new material has been come out to be 10.25 with a loss tangent of 0.002. The dielectric constant of its counterpart material viz FR4 and RO3006 are 4.4 and 2.2. The tensile modulus and stress demonstrated by this new material are 189 Kpsi and 50 MPa respectively. The new dielectric material. The customised material has been named as TB-11. TB-11 will find numerous applications and use cases as it is further developed and made commercially available.

The copper cladding of the TB-11 material was carried out with the support of M/s Transline Technologies, USA; and the designing and testing of the patch antenna was carried out at Sahajanand Laser Technology Limited (SLTL), Gandhinagar, Gujarat. The three types of patch antenna were designed, tested and evaluated at

SLTL. The gain and S-parameter of the array antenna with TB-11 are found to be 14 dB and -19.3 dB respectively which are more than the values obtained with FR4 and RO3006 material. The gain and S-parameter with FR4 and Ro3006 are 11 dB, 12.5 dB, -14.7 dB and -16.4 dB respectively. The sensors were fully fabricated and the entire system was implemented and tested on the river site in Ahmedabad. The results obtained are encouraging and demonstrated that human and non-human intrusions can be detected.

Acknowledgement

I sincerely thank Vice Chancellor and Dean of University of Petroleum and Energy Studies for all the logistics and facilitation during the journey of my studies and research.

I am fortunate to have a very able, thorough professional and wonderful person like Prof. Dr. Piyush Kuchhal as my guide. Similarly, I am guided by Dr. Kanhiya Lal, a giant personality and innovator in the field of microwave based products. He is the motivator to venture into ‘unachievable’ achievements by helping to design the Indigenous and enhanced dielectric material, and the patch antenna.

I sincerely thank Sahajanand Technologies Limited and Shri Arning Patel/ MD for providing the facility for the real world testing of the dielectric materials and the new patch antennas. I also thank Shri Virendra Singh/ Sr Microwave designer/ SLTL for continuing support and being co-author in my publications.

I thanks Dr. Ranjan Mishra for the continued support and motivation throughout the research. I sincerely thank Dr. NN Jani/ Former Dean and Prof. and Dr. Prof. Richa Mehta of Kadi Sarva Vishva Vidyalay, Gandhinadar.

I thank Shri Lalit Padmani and M/S Transline Technologies, USA for copper cladding on TB-11 dielectric sheets, fabricating the patch array antennas on TB-11, Roger RO3006 and FR4 material. I thank Teksun Microsys (P) Limited for the logistics and support for my research. I also take the opportunity to thank Miss Suhani Patel/ Jr. Data scientist, Shri Hardik Choudhry, Shri Suraj Shethia of Teksun Microsys and Ms. Hemangi Patel/ Reve Automation LLP for their continuing support in the experiments carried out during the research.

I sincerely thank Shri DB Bhatt/ Sr. Scientist/ Engineer SAC/ ISRO for helping in selecting the frequency band for the ‘coastal line intrusion detection application. I also thank the officials of India Coast Guard for helping me to understand the domain and the site conditions. I thank Prof. Dr. Malkesh Patel, Ms. Priyanka Bhatnagar of “Incheon National University, South Korea” and Ms. Shristi Bits for their active support throughout my research.

I thank the Institution of Electronic and Telecommunications Engineers for providing the library facility, guidance and support. I also thank M/S Jyoti Electronics for providing extensive support in the design and simulations of patch antennas using different dielectric materials.

I thank Green Field Control Systems, Green Cloud iSoft and their officials for providing the facility and logistics.

I thank one and all who have directly or indirectly helped me during the journey of research.

Lastly, I also thank Ms Rakhee Ruyal and all the team of SRE, UPES for supporting me during the research.

Contents

Abstract	i
Acknowledgement	iv
List of Figures	x
List of Tables	xii
1 Introduction	1
1.1 Antenna and its types	2
1.1.1 Classification in Terms of Wire Structure	2
1.1.2 Classification in Terms of Aperture Structure	3
1.1.3 Classification in Terms of Frequency	4
1.2 Antenna Characteristics	5
1.2.1 S-Parameter	5
1.2.2 VSWR	6
1.2.3 Bandwidth	7
1.2.4 Gain	7
1.2.5 Directivity	8
1.2.6 Antenna Efficiency	9
1.3 Antenna Pattern	10
1.3.1 Omnidirectional Antenna	10
1.3.2 Directional Antenna	11

1.3.3	Isotropic radiator	11
1.3.4	Field Regions	12
1.3.5	Antenna polarization	12
1.4	Microstrip Antenna	13
1.4.1	Applications of Microstrip Antennas	14
1.5	Microstrip Antenna Structure	15
1.6	Feeding Techniques for Microstrip Antenna	17
1.6.1	Microstrip Line Feed	18
1.6.2	Coaxial Probe Feed	19
1.6.3	Aperture Coupled Microstrip Feed	20
1.6.4	Proximity Coupled Microstrip Feed Technique	21
1.6.5	Coplanar Wave Guide Feeding	22
1.7	Research Objectives	23
2	Literature Review	25
2.1	Literature Survey	25
2.2	Chapter Summary	42
3	Design, Fabrication and Testing of Proposed Substrate SLTL-TB11	43
3.1	Needs of customized Substrate material	44
3.1.1	FR4	44
3.1.2	Roger RO3000	45
3.2	New Dielectric Substrate Material Composition STTL-TB11	46
3.2.1	Butyl Rubber	46
3.2.2	Titanium dioxide (TiO ₂)	47
3.2.3	Butyl Rubber-SrTiO ₃	48
3.3	The proposed Substrate SLTL TB-11	49
3.4	Testing Method	50
3.5	Chapter Summary	52

4	Antenna Array Design Using Different Substrate	53
4.1	Design Specifications	53
4.1.1	Dimension of Patch Antenna	54
4.1.2	Dimension of Substrate	55
4.2	Design of Microstrip Patch Antenna Array using FR4 substrate . . .	56
4.2.1	Simulation Results and Discussion	56
4.2.1.1	S11 Parameter and Bandwidth	56
4.2.1.2	Voltage Standing Wave Ratio (VSWR)	57
4.2.1.3	Gain	58
4.2.1.4	Radiation pattern	58
4.3	Design of Microstrip Patch Antenna Array using RO-3006	58
4.3.1	Simulation Results and Discussion	59
4.3.1.1	S11 parameter and bandwidth	59
4.3.1.2	Voltage Standing Wave Ratio (VSWR)	60
4.3.1.3	Gain	61
4.3.1.4	Radiation pattern	61
4.4	Design of Microstrip Patch Antenna using Substrate SLTL-TB11 . . .	61
4.4.1	Simulation Results and Discussion	62
4.4.1.1	S11 Parameter and Bandwidth	62
4.4.1.2	Voltage Standing Wave Ratio (VSWR)	63
4.4.1.3	Gain	64
4.4.1.4	Radiation pattern	64
4.5	Comparison of Antenna array results obtained three substrate	64
4.6	Fabrication of Antenna Array using SLTL-TB11 substrate	65
4.7	Testing of the SLTL-TB11 Antenna Array	66
4.8	Validation of the simulated result with measured results	68
4.9	Chapter Summary	69

5 Coastal Surveillance Application of the Proposed Antenna Arrays	71
5.1 Test setup and Data collection	72
5.2 Gain and Distance Calculations	74
5.3 Results and Discussion	76
5.3.1 Safety considerations	77
5.4 Summary of chapter	77
6 Conclusion and Future Work	79
6.1 Conclusion	79
6.2 Future Scope	81
Bibliography	82
Publications	93
Scholar's Resume	94
Plagiarism Certificate	97

List of Figures

1.1	Geometry of a Microstrip Antenna	16
1.2	Different feeding techniques	18
1.3	Microstrip Antenna fed by Microstrip Line Feed	19
1.4	Microstrip Antenna fed by Coaxial Probe Feed	20
1.5	Microstrip Antenna fed by Aperture Coupled Microstrip Feed	21
1.6	Microstrip Antenna fed by Proximity Coupled Microstrip Feed	22
1.7	Microstrip Antenna fed by Coplanar Wave Guide Feed	22
3.1	Fabrication process of proposed substrate	50
4.1	Schematic representation of One element of patch antenna	55
4.2	Schematic representation of 8x1 Antenna Array	56
4.3	S11 parameter of FR4 for Microstrip feed Array.	57
4.4	VSWR of FR4 Antenna Array	57
4.5	Gain of FR4 Antenna Array	58
4.6	Radiation Pattern of FR4 Array Antenna	59
4.7	S11 parameter of RO3006 Antenna Array	60
4.8	VSWR of of RO3006 Antenna Array	60
4.9	Gain of RO3006 Antenna Array	61
4.10	Radiation pattern of RO3006 Antenna Array	62
4.11	S11 of Antenna Array using SLTL-TB11	63
4.12	VSWR of Antenna Array using SLTL-TB11	63
4.13	Gain of Antenna Array using SLTL-TB11	64

4.14	Radiation pattern Antenna array using SLTL-TB11	65
4.15	Comparison of Gain and Beamwidth of antenna array	66
4.16	Fabricated Image of Antenna array along with Researcher	67
4.17	A close image of the fabricated SLTL-TB11 array antenna	67
4.18	Validation of S11 parameter of antenna array using SLTL-TB11	68
4.19	Validation of Gain of antenna array using SLTL-TB11	69
5.1	Schematic block of Test setup to capture intruder data	72
5.2	Block diagram illustrating the functioning of Transmitter	73
5.3	Block diagram illustrating the functioning of Receiver	73

List of Tables

3.1	strain-stress characteristics of Butyl rubber	47
3.2	Microwave, physical and thermal properties of TiO ₂ [84,85]	48
3.3	Parametric comparison of FR4, RO3006 and Customised substrate TB-11	51
4.1	Design Parameter of array antenna using FR4	56
4.2	Design Parameter of array antenna using RO3006	59
4.3	Design Parameter of Antenna Array using SLTL-TB11	62
4.4	Result characteristics of the antenna array using three substrates . . .	65
4.5	Result of the simulated and measured work of Antenna array using SLTL-TB11 substrate	69
5.1	Drop in Received Power Level (in dB) against the movement of intruder	78

Chapter 1

Introduction

Because of their flexibility and capability of providing precise and heterogeneous measurements of parameters that describe the marine environment, especially in coastal areas, sensors are now widely used for coastal monitoring. Indeed, the ability of these sensors to measure coastal phenomena (waves, currents, plumes, morphology, and so on) in real time and with high accuracy makes them particularly valuable in enhancing understanding of the dynamic evolution of coastal phenomena. Examples include a proper knowledge of the consequences of severe weather conditions on coastal morphodynamics and real-time monitoring of contaminant spills.

India has a long coastline (7516 km) with a thriving fishing sector that relies on the resources of the sea. As previous occurrences have demonstrated, effective surveillance with tracking of the coast is important to maintain the nation's security and economic strength. The Integrated Control and Safety System (ICSS) programmed is being undertaken to develop an indigenous solution that covers the entire coastal line and to provide integrated coastal surveillance using the in-house sensors and communication technologies available with the Defence Research and Development Organisation (DRDO) to improve maritime domain awareness and decision-making capabilities. The installation of a variety of various types of surveillance sensors along the shore to provide year-round monitoring during all seasons is required. The electromagnetic sensor may play important role to detect the intru-

sion along the coastal line

Electromagnetic waves interact with materials in a variety of ways. It is determined by the radiation's power, frequency, and the properties of the physical medium with which it interacts. As a result, electromagnetic waves of varying frequencies interact differently with the medium in which they propagate. This interaction can be studied in the receiver by monitoring the signal's characteristics (frequency, amplitude, and phase). Electromagnetic characteristics characterise matter and can be utilised to detect it. Distinct frequency and matter parameters (conductivity, permittivity, and permeability) cause different interaction mechanisms: the medium can be evaluated after the interaction by measuring in the receiver.

1.1 Antenna and its types

An antenna is required for a radio wireless device to function [1]. Using a transmit antenna, you can take a signal from a transmission line and transform it into electromagnetic waves, which you can then broadcast into the universe. A receive antenna is located at the other end of the link and is responsible for collecting the incident electromagnetic waves and converting them back into signals.

An antenna can be classified in terms of its wire structure, aperture configuration and frequency usage. [2]. The wire antenna is the most basic of the antennas that was used for a long period. This is the early developed antenna structure, used in tall building, and considered to be simpler and less expensive.

1.1.1 Classification in Terms of Wire Structure

In terms of wire structure there are three types of antennas as stated below.

- Dipole or Linear Wire Antenna - A dipole antenna, also known as a linear wire antenna, is an antenna that is made out of straight wires.
- Loop Antenna - A loop antenna is a type of antenna in which a single wire is used to form a loop around another wire. The loop can take on any shape, although the most common shapes are circular and square, which are employed mostly for the convenience of analysis and construction.
- Helical Antenna - An antenna in which the wire has been bent into a helical shape is called a helical antenna. It is referred to as a helix antenna in some circles.

1.1.2 Classification in Terms of Aperture Structure

Another type of categorization is based on the aperture structure of the antenna. the aperture is the outer flare of the antenna. It is a two-dimensional surface on which to operate. Patch antenna is one of its category and this is the base design of this research work. The various antennas that fall under this category are as follows:

- Horn Antenna - This antenna is made from waveguide. A waveguide is a hollow metallic tube that is used in radio communications. The cross-section of the waveguide, through which the waves propagate, determines the shape of the horn antenna, and vice versa. When one end of a waveguide is trapped in a big opening and works as an antenna, the waveguide is said to be inductively coupled.
- Parabolic Disc Antenna - It is possible to design an antenna in the shape of a parabolic or disc. It is mostly employed for very long-distance receiving as well as for space reception applications. They've also referred to it as a reactor antenna.

- Microstrip Antenna - It is also known as patch antenna. In this structure, a radiating patch that has been carved into the substrate. The metallic ground plane is located on the opposite side of the substrate.
- Array Antenna - A multi-element antenna has many elements. Whenever a single element is unable to provide the needed attributes, they are used to supplement the situation. The use of multiple elements in the antenna structure allows for the achievement of the necessary characteristics.

1.1.3 Classification in Terms of Frequency

Frequency is the most essential and important characteristics in communication. For this reason, in terms of frequency-specific classes, the antenna is categorized as follows:

- Very High Frequency (VHF) Ultra High Frequency (UHF) Antennas: The frequency range of VHF is 30 MHz to 300 MHz, and the frequency range of UHF is 300 MHz to 3 GHz. The antennae that operate at this frequency include Yagi-Uda antennas, log-periodic antennas, Helical antennas, Panel antennas, Corner sector antennas, parabolic antennas, disconnect antennas, and other similar designs.
- Super High Frequency (SHF) Extremely High Frequency (EHF) Antennas: The frequency in this region is greater than 3 GHz. Microwave antennas are another name for these two frequency regions. A variety of antenna covers are available, including parabolic antennas, pyramidal horn antennas, disconnect antennas, monopole and dipole antennas, Microstrip patch antennas, fractal antennas, and others.

1.2 Antenna Characteristics

An antenna makes a radio frequency communication device possible. When used on the transmission side, it receives an electrical signal from a transmission line, converts it into electromagnetic waves, and then broadcasts the electromagnetic waves into free space [3]. The receiving end of the transmission is where it takes the electromagnetic waves that have been transmitted and turn them back into an electrical signal. The characteristics of an antenna are usually done based on different parameters. These parameters are defined based on electromagnetic field radiated by the antenna. The radiation pattern of the antenna can be determined from the radiated fields, and it can be used to design the antenna, the various properties are quantized.

The antenna must undergo various measurements. There are two types of measurement: passive measurement and active measurement [9]. It is necessary to quantify passive parameters such as return loss, voltage standing wave ratio (VSWR), and impedance bandwidth. The active measurement of antenna parameters covers the radiation pattern, gain, efficiency, and directivity of the antennas, among other things. The fundamental parameters for the antenna are listed below:

1.2.1 S-Parameter

S-parameters are used to characterize the relationship between the input and output of a system between two ports or two terminals. S-parameters are exclusively the function of frequency and it varies with the frequency. In a general system if two ports are represented by port A and port B, then the power transferred from port B to port A is describe as S_{AB} .

S_{11} , also known as return loss or reflection coefficient, is then denoted as the reflected power in the port as it delivers power to the antenna throughout the transmission process. S_{11} is a measure of the amount of power that is reflected at the antenna as a result of a mismatch between the antenna and the transmission line. For an S_{11} value of 0 dB, all the power is reflected by the antenna. More is the

negative value of S11 better will be the antenna performance. As a result, the bulk of the power sent to the antenna is radiated into free space because the majority of the antennas are designed to be a low loss. The reflection coefficient is the ratio of the transmitted voltage to the reflected voltage. Therefore the return loss or the power fraction reflected (S11) is proportional to the reflection coefficient squared.

1.2.2 VSWR

It is a numerical representation of how well a specific is matched with the transmission line that is attached to the antenna. For a transmitter, the impedance must be well matched to the impedance of the antenna. Its value varies from 1 to infinity. The smaller the value better is the matching of the antenna with the longer the input line, the greater the amount of power sent to the antenna by the line. VSWR equal to 1 result in 100 percentage radiation and zero reflection of the power source.

VSWR is a frequently used parameter to characterize impedance matching. In the standing wave pattern at an impedance discontinuity, it is defined as the ratio of the peak voltage maximum to the peak voltage lowest at the impedance discontinuity. This is also regarded as the variation in the amplitude of the standing wave envelope. VSWR is related to the reflection coefficient in the following ways:

$$VSWR = \frac{1 + |\Gamma|}{1 - |\Gamma|} \quad (1.1)$$

$$\Gamma = \frac{Z_{in} - Z_o}{Z_{in} + Z_o} \quad (1.2)$$

here, Z_{in} and Z_o are the input and normalized impedance of the terminal. And, the return loss, $R_L = -20\log\Gamma$. For a perfect matching, there is no reflected signal and VSWR.

1.2.3 Bandwidth

It is fundamental and desired to determine a parameter of the antenna. An antenna's bandwidth is defined as the range of frequencies over which it can transmit or receive electromagnetic radiation while still maintaining a constant return loss. It is also referred to as the impedance bandwidth. Because the impedance of an antenna varies with frequency, the antenna is matched with the line within a limited range of frequencies. This range of the frequencies defined the bandwidth of the antenna. The bandwidth is paired with a Return Loss or VSWR value. It is the ratio of bandwidth to the central frequency that determines a system's fractional bandwidth (BW). The bandwidth and percentage bandwidth are calculated as

$$BW = f_H - f_L \quad (1.3)$$

$$BW\% = 2 \frac{f_H - f_L}{f_H + f_L} * 100 \quad (1.4)$$

1.2.4 Gain

Gain is defined as the difference between the amount of power transferred in the direction of peak radiation and the amount of power sent by an isotropic source. Gain is measured in watts. According to this definition, a gain of 3 dB means the power received from this antenna would be 3 dB more than the power received from a lossless isotropic antenna with the same input power. Gain is also defined as the ratio between maximum radiation intensity to the total input power.

$$G = \frac{\text{maximum radiation intensity}}{\text{total input power}} \quad (1.5)$$

In terms of efficiency of the antenna,

$$Gain = \frac{E_r 4\pi |U(\theta, \phi)|_{max}}{P_{rad}} = \frac{E_r}{D} \quad (1.6)$$

Gain (in dB) = $G_{dB} = 10 \log G$. An ideal isotropic antenna ($\eta \approx 1$) has a gain

of 0 dB. Here the transmitted power is uniformly distributed over the area of a spherical shell at a particular range (R) from the antenna.

Thus, the radiated power density (S) is given as:

$$S = \frac{P_t G_t}{4\pi R^2} \quad (1.7)$$

Here P_t and G_t are the transmitted power and transmitted antenna's maximum gain.

Whereas, the Effective Isotropic Radiated Power (EIRP) is defined as:

$$EIRP = P_t G_t \quad (1.8)$$

The Effective Aperture (A_e) of an antenna in the region that it can effectively collect. It is the area of an incident wavefront that the antenna can be intercepted. It is defined in terms of gain and wavelength.

$$A_e = \frac{G^2}{4\pi} \quad (1.9)$$

1.2.5 Directivity

The capacity of an antenna to focus radiation is referred to as directivity. This term describes the measurement of its directional property. It applies only to the directional properties of the antenna and is controlled by the radiation pattern. The directivity of an antenna is one if it radiates in all directions in an equal and uniform manner. It has effectively zero directionality. The Directivity (D) of an antenna is the ratio of how much energy it directs in a particular direction divided by the average energy. The directivity of an isotropic antenna is 1.

$$D = \frac{\text{Peak Energy}}{\text{Average Energy}} \quad (1.10)$$

Directivity and gain are related to efficiency (η). Efficiency is the ratio of the

radiated power and the input power.

$$\eta = \frac{P_{rad}}{P_{in}} = \frac{Gain}{Directivity} \quad (1.11)$$

Decibels are commonly used to express the gain of an antenna concerning the gain of an isotropic antenna. The difference between gain and directivity is the concept of denying the power describe mathematically. For a lossless antenna, the gain is equal to directivity since the input power delivered to it is the same as the output power radiated away from the antenna. i.e. $P_{rad} = P_{in}$. Therefore, in this case, the gain is equal to directivity.

1.2.6 Antenna Efficiency

An antenna can transmit input power into the radiation. It relates the power delivered to the antenna with the dissipated within the antenna. It shows how well an antenna transmits the accepted input power to the output radiated power. Because of the impedance mismatch between the antenna and the environment, an antenna with high efficiency radiates the majority of its power into free space, whereas an antenna with low efficiency absorbs or reflects away the majority of its power. The antenna efficiency can be defined as the ratio of the radiated power to the input power of the antenna. It also relates the gain of the antenna with its directivity. An efficient antenna transmits most of its power into the free space as radio waves.

$$\text{Radiation Efficiency} = \frac{\text{Power Radiated}}{\text{Power Input}} = \frac{\text{Gain}}{\text{Directivity}} \quad (1.12)$$

Total efficiency is the antenna's radiation efficiency multiplied by the antenna's impedance mismatch loss gives the total radiation efficiency of the antenna. Since the impedance mismatch loss varies from 0 to 1, the total efficiency is always less than the radiation efficiency. For a perfect matching, the two efficiencies are the same.

1.3 Antenna Pattern

An antenna pattern is a measurement of the angle of view provided by an antenna. It depicts the spatial distribution of the energy radiated or received by the antenna and is used in antenna design. The broad opinion is that of an isotropic antenna. More practical is omnidirectional antenna though for some purposes directional antenna is preferred. An examination of the orientation and arrangement of the antenna elements reveals the orientation of the electric fields. The anisotropic antenna is the one that radiates and receives energy uniformly in all directions. A true isotropic antenna is a topological impossible because electromagnetic waves are transverse.

An omnidirectional antenna, often known as an Omni-antenna, radiates and receives energy in all azimuthal directions in the same manner. An Omni-pattern may be readily achieved. They need the energy in a particular plane. Dipole and small loop antenna are examples of Omni-antenna.

Directional or gain antennas focus energy in a particular narrow field of view. It is ideal for a point-to-point link or any other application where the antenna is aligned to aim directly at the other end of the link. Horn antenna, dish antenna, and reflectors are typical examples of it. An antenna radiation pattern function, the angular distribution of the energy radiated or received by the antenna is described by this term. The half-power, or -3 dB, locations on an antenna's field of vision are the most restrictive. The half-power bandwidth of an antenna is defined as the angular measure between the -3 dB points.

The common terms associated with the radiation patterns are as follows:

1.3.1 Omnidirectional Antenna

In radio communications, an omnidirectional antenna is defined as an antenna with a radiation pattern that is homogeneous and evenly dispersed in a single plane, which is sometimes referred to as the horizontal plane. Some applications, such as

mobile phones, cell phone towers, FM radios, walkie-talkies, wireless computer networks, cordless phones, GPS, and many portable handheld devices, as well as base stations, necessitate the use of antennas with characteristics that radiate equally in all directions in a plane

The radiation pattern of an omnidirectional antenna resembles a doughnut. Among the many types of low gain, omnidirectional antennas that can be found are slot antennas and dipole antennas, whip antennas, disconnect antennas, and the duck antenna, among others. By narrowing the beamwidth of the antenna in the vertical plane, we can improve performance, it possible to design an omnidirectional antenna with a high gain. This will result in the concentration of energy in the horizontal plane, which may be used to create an omnidirectional antenna. Due to the high gain of a small beamwidth antenna, numerous types of omnidirectional antennas with varied strengths can be designed. Vertical plane radiation is more efficient when using a 0 dB gain antenna.

1.3.2 Directional Antenna

Radiation from directional antennas is concentrated in a specific direction, as implied by the name. They are also referred to as Beam Antennas in some circles. They are beneficial in some point-to-point applications such as satellite communication, in base station antennas for transferring energy in a specified sector, and some other uses, and in a variety of other applications as well. Some examples of directional radiation pattern antennas are the Yagi antenna, horn antenna, log-periodic antenna, and panel antenna, to name a few of the types.

1.3.3 Isotropic radiator

The anisotropic antenna is one in which the radiation is dispersed evenly in all directions over the whole spectrum. The anisotropic antenna radiates the entire amount of power that is applied. It is a fictitious antenna that does not exist in the real

world. It is used as a baseline for comparing the performance of the other antennas.

1.3.4 Field Regions

The intensity of the radiations radiated by an antenna changes as we travel away from the source of the radiations. One can distinguish between the Far Field (Fresnel) region and the Near Field (Fresnel) region, which are two different types of field regions. The far-field region is defined as the area beyond the Fraunhofer distance, often known as the Fraunhofer region, which is a geographical region in Germany. It is important to note that the radiation pattern does not change with distance at this place, and it does not vary with distance at this position. The Fraunhofer distance is proportional to the bigger diameter of the antenna.

1.3.5 Antenna polarization

It is the polarisation of electromagnetic waves that emanate from an antenna that determines the polarisation of the antenna. The direction in electrical engineering, polarisation refers to the route traces traced by an electric field vector on a wave as a function of time. Generally speaking, polarisation can be divided into three categories.

- Linear polarization
- Circular polarization
- Elliptical polarization

In electromagnetic waves, a linear path is defined as follows: if an electric field vector of the wave at a particular location in space follows a straight line, the polarisation is linear. Linguistic polarisation can be divided into two types: vertical polarization and horizontal polarisation. Circular polarisation produces an electric field vector that follows a circular path, while elliptical polarisation produces an electric field vector that follows an elliptical path. Electric fields with left-hand polarisation are

possible if the electric field vector tracking the path rotates in a clockwise direction, and electric fields with right-hand polarisation are possible if the electric field vector tracking the path rotates in an anti-clockwise direction. Left hand polarised electric fields are also possible if the electric field vector tracking the path rotates in a clockwise direction.

1.4 Microstrip Antenna

Microstrip antennas are also termed as patch antenna and it is one of the most important classes of antennas in microwave communication. The creation of unique microwave antenna designs and technologies is the most significant undertaking in the development of microwave communication systems that meet the appropriate radiation parameters. As a result of its ease of use and compatibility with printed circuit technology, it is more popular in wireless communication systems these days. Microstrip geometries that transmit electromagnetic waves were first proposed in the 1950s and have now gained widespread acceptance. Deschamps was the first to suggest the notion of a microstrip antenna, which occurred in the year 1953 [4]. In the year 1955, Button and Baissinot submitted a patent application for the microstrip antenna.

Microstrip lines and radiators were developed as specialized devices in laboratories in the early days. During this period, there were no commercially accessible printed circuit boards with regulated dielectric constants produced or introduced. As a result, it wasn't until the 1970s that Robert E. Munson's antenna [5] became viable after further development by him. Other researchers were able to speed development throughout this decade as a result of the availability of low-loss tangent substrate materials at the time. Improvements in photolithographic processes enhanced theoretical modeling, and the attractive thermal and mechanical qualities of the substrate are all contributing factors to the advancement of the technology.

Munson and Howell [6] were responsible for the development of the first workable antenna. The substantial study and development of microstrip antennas and arrays that have taken place since then have resulted in a wide range of applications in the broad field of microwave antenna technology. Recently developed printed circuit technology has allowed microstrip or printed patch antennas to be employed in practically all wireless systems, making them more widely available. In wireless communication applications, the objective of a microstrip or patch antenna is to radiate and receive electromagnetic energy in the microwave range, and it plays a vital role in this process. For a microstrip antenna to perform and operate properly, it must have a specific shape and be made of a material with specific qualities [7].

1.4.1 Applications of Microstrip Antennas

The usage of microstrip or printed patch antennas can meet a wide range of commercial applications, and they are becoming increasingly popular. Patch antennas come in a variety of designs, although rectangular-shaped patch antennas are the most often utilized. In mobile and satellite communication systems, a microstrip patch antenna meets or exceeds the majority of the criteria, and many different types of microstrip antennas are available for this purpose. Aside from these and other prominent applications such as aircraft, spacecraft, satellites, and missiles, the employment of microstrip antennas is particularly well suited because of their small size and weight, low cost, high performance, ease of installation, and low-profile nature. Additionally, there are other governments and commercial uses in the areas of mobile radio and wireless communications where the use of this antenna is appropriate, such as public safety communications.

Some significant applications for which microstrip antennas have been developed and found to be appropriate in Satellite Communication Direct Broadcast Service, Mobile Communication Systems, Doppler and other Radars, Telemetry, Remote Sensing & Environmental Instrumentation, Satellite Navigation Receivers, Radio Altimeter, Biomedical Radiators and Intruder Alarms, and Personal Wireless Com-

munication Systems and Service [9].

It is possible to meet a significant number of business requirements through the usage of these antennas. The omnipresent Global Positioning System (GPS), ZigBee, Bluetooth, WiMax, Wireless Fidelity (WiFi), and wireless communication systems are only a few of the technologies used in many applications. Antennas are in high demand due to navigational applications such as asset tracking for automobiles and maritime applications, among other things. It is widely used in radio frequency identification (RFID) and radar systems in the fields of manufacturing, transportation, and medicine, among other applications. In a nutshell, microstrip antennas meet the needs of an antenna system that is both flexible and light in weight. In recent years, printed monopole microstrip antennas have been utilized in Satellite Digital Audio Radio Services, which serve as an alternative to audio commercial broadcasts in automobiles and are becoming increasingly popular [10]. Aspects of communication systems that benefit from the usage of antennas will continue to spur the development of new applications that rely on their utilization. In current society, they are the gadget that enables all of the wireless technologies that have become so commonplace and omnipresent. Because of the high material costs of cable infrastructure, antennas are increasingly being used in many modern communication systems. The number of applications for Microstrip antennas will continue to develop as people become more aware of the possibilities offered by this technology, which is particularly advantageous due to its radiation mechanism and functional performance. When it comes to particular applications in communications, electronic support, and countermeasures, radar, and radiometry, a large amount of available bandwidth is necessary.

1.5 Microstrip Antenna Structure

The most fundamental form of a Microstrip patch antenna, which is composed of a radiating patch mounted on one side of a dielectric substrate [2] and a ground plane

mounted on the other side is illustrated in Figure 1.1.

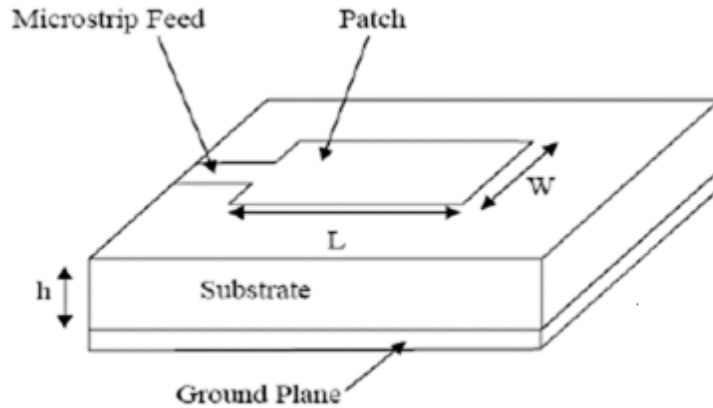


Figure 1.1: Geometry of a Microstrip Antenna

A microstrip antenna is a dielectric substrate panel placed between two conductors, which is its most basic configuration. The lower conductor is referred to as the ground plane, whereas the upper conductor is referred to as a patch. The frequency range for microstrip antennas is between 1 GHz and 100 GHz, which is the most commonly utilized range. The patch has been chosen since it is quite thin. Patches are typically composed of precious metals such as gold or copper and can be designed in any shape. These conducting metals are the most commonly used because of their low resistivity, resilience to oxidation, ease of soldering, and ability to attach well to a variety of surfaces. In this case, the dielectric substrate is used to etch the feed line and radiating patch.

In addition to other forms and sizes, the MA radiating patch can be any shape or size. Examples include squares, triangles, rectangles, circles, and ellipses as well as segmental oval and annular rings, among other shapes and sizes. The rectangular microstrip antenna (MA) is the most commonly used MA due to the ease with which it can be developed, fabricated, and characterized for research purposes, among other factors [11].

To achieve the appropriate qualities, the radiating patch can be built in a variety of shapes. Due to their ease of production and analysis, circular, square, and rectan-

gular designs are the most commonly used. Although their geometrical shapes are different, their radiation characteristics are very similar because they behave like a dipole. When the thickness of the dielectric substrate is increased, the surface waves and spurious feed radiation become more prominent, resulting in a reduction in the antenna's bandwidth. Cross-polarized radiation is produced as a result of the feed radiation, which is undesirable. The use of a thick dielectric substrate with a low dielectric constant is beneficial for improved performance in electrical applications. Improved efficiency and radiation will result as a result of this. However, this characteristic has the effect of increasing the size of the antenna. The dielectric constants of the substrate should be high to build a compact structure. Such a design, on the other hand, will be less efficient and will have a smaller bandwidth.

To secure the maximal transfer of energy from the source to the radiating elements, impedance matching between the antenna and the feed line is required. The matching between the antenna and the feed line will be provided by a port location that has been roughly selected.

1.6 Feeding Techniques for Microstrip Antenna

For electromagnetic radiation to travel from the source to the region under the patch, the feed must be guided. Some of this energy escapes the patch's confines and is emitted into the surrounding space.

Feeding methods can be divided into two categories: those that involve contact and those that do not involve contact. A connecting device like a microstrip line, for example, is used to direct the radio frequency power from the input to the patch when using the contacting method [12]. It is done by electromagnetic field coupling to transmit power between the microstrip line and the radiating patch in the non-contacting method, which is commonly referred to as an indirect scheme by some. The microstrip line feed, coaxial feed, aperture coupling feed, proximity coupled microstrip feed, and coplanar waveguide feed are the four most prominent feed systems used in semiconductor manufacturing. Varied feeding methods in science

produce different antenna features, including bandwidth, radiation pattern, polarization, gain, and impedance, among other things. Feeding methods such as coaxial and microstrip feeding are the most frequently encountered in practice. Because the input impedance of the antenna differs from the standard 50-ohm line impedance, matching is frequently necessary between the antenna and the feed lines. The matching between the antenna and its feed line will be achieved by placing the port in the proper location on the antenna [13].

A variety of ways are available for coupling power into or out of a microstrip antenna, which can be broadly classified into two categories: contact (direct) feed and non-contact (indirect) feed. As illustrated in Figure 1.2, these two approaches are further subdivided.

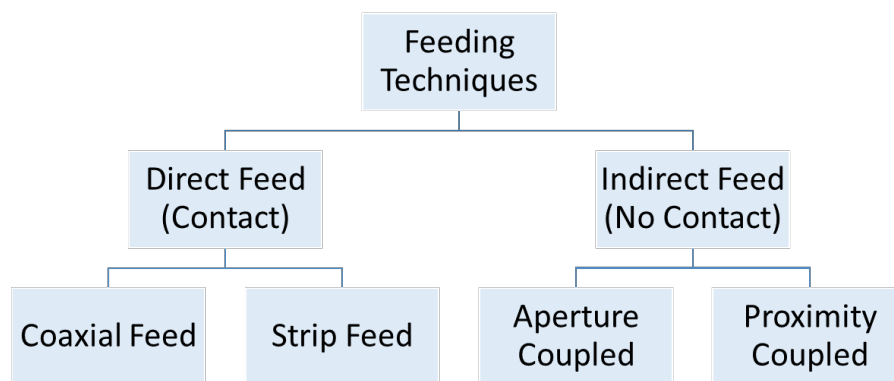


Figure 1.2: Different feeding techniques

1.6.1 Microstrip Line Feed

An electrically conductive strip is linked directly to the edge of the Microstrip patch in this type of feed approach as illustrated in Figure 1.3 .When comparing the width of the conducting strip and the size of the patch, the conducting strip is smaller. Since this feeding arrangement and a radiating patch can both be printed on the same dielectric substrate, this method is the most straightforward to construct . The planar structure provided by this design is advantageous. Furthermore, in the mm-wave area of the spectrum, the size of the feed line is the same as the size of

the patch size, increasing unwanted radiation. In addition, an inset incision in the patch may be included in the feed arrangement to the patch. Because of the inset cut in the patch, the impedance of the feed line can be matched to that of the patch without the use of an additional matching element. This is accomplished by the use of correct control of the inset position. Due to the ease of fabrication and modeling, as well as the simplicity of impedance matching, this is a simple feeding scheme to implement and maintain.

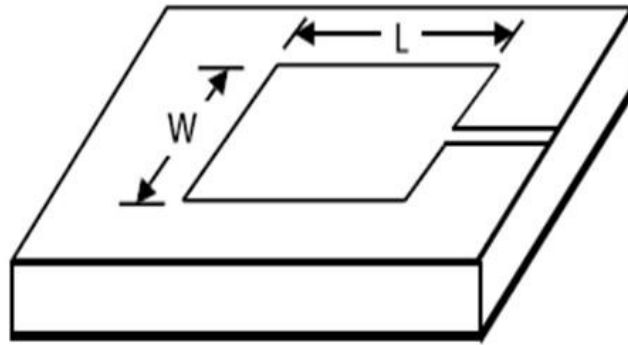


Figure 1.3: Microstrip Antenna fed by Microstrip Line Feed

1.6.2 Coaxial Probe Feed

The coaxial feed, often known as the probe feed, is the most widely used approach for feeding printed patch antennas. Depending on the impedance matching requirements, this feed can be placed anywhere within the patch. The inner conductor of the coaxial connector extends through the dielectric and is attached to the radiating patch, whilst the outside conductor is linked to the ground plane of the device being connected to. The illustration of this method is shown in Figure 1.4. The coaxial feed method, also known as probe feed, has a low radiation loss. In terms of advantages, the key advantage of this feed is that it may be positioned at any desired point within the patch to match the input impedance of the patch. This feed mechanism is simple to construct and emits a low amount of spurious radiation. Nonetheless, its primary disadvantage is that it provides less bandwidth and is more

difficult to implement because a hole must be drilled into the dielectric substrate.

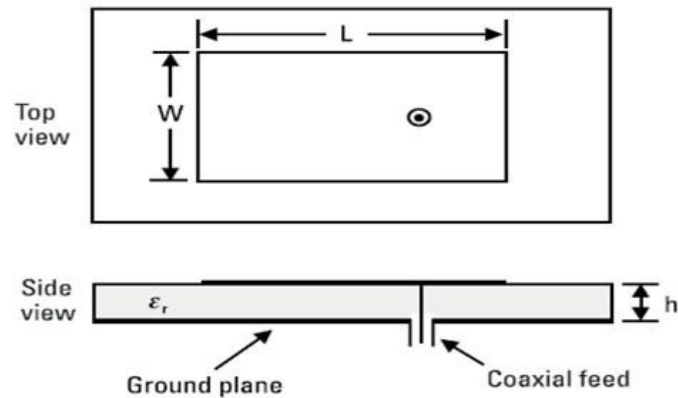


Figure 1.4: Microstrip Antenna fed by Coaxial Probe Feed

The microstrip line feed and the coaxial feed suffer from the difficulties of probe reactance and surface wave excitation when operating on a dielectric substrate with a significant thickness. The indirect feed, as mentioned further below, provides a solution to these issues.

1.6.3 Aperture Coupled Microstrip Feed

When a slot in the ground structure is inserted between the two substrates of the system, then it is connected from the feed line to the resonant patch, resulting in an aperture coupling between the two substrates of the system as illustrated in Figure 1.5. On this board, there is a feed line on the bottom substrate and a radiating patch on the top substrate, both of which are copper. The coupling aperture is almost always located beneath the patch in the majority of cases. As a result of configuration symmetry, this leads to the reduction of cross-polarization in the system. The aperture in the feed line and the patch, as well as the shape, size, and location of the aperture, determine the amount of coupling that occurs between the two components. Resonant or nonresonant characteristics of the slot aperture can be achieved depending on the application.

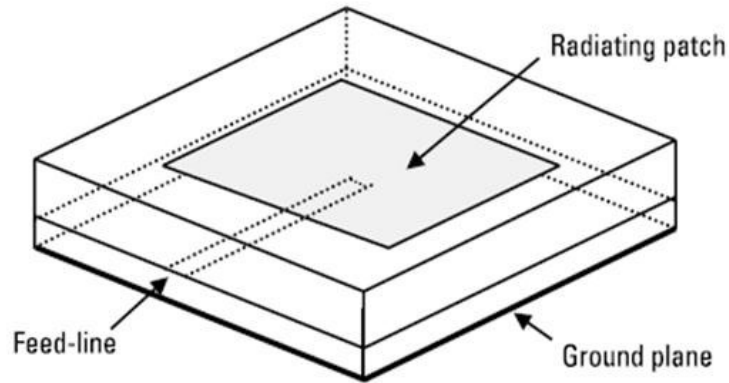


Figure 1.5: Microstrip Antenna fed by Aperture Coupled Microstrip Feed

1.6.4 Proximity Coupled Microstrip Feed Technique

A two-layer substrate with the microstrip line on the lower layer and the patch antenna on the upper layer was employed for a con duration of this non-contacting microstrip feed. One of the dielectric layers in this feeding approach is a radiating patch layer, and the other is a lower layer feed line that has been created with a ground plane on the backside of the device. A common ground plane separates the two substrates from one another. The patch is electromagnetically related to the bottom substrate's microstrip feed line, which is connected to the patch through a slot aperture in the common ground plane. The arrangement is illustrated in Figure 1.6. Because of the shielding effect of the ground plane, the radiation from the open end of the feed line does not interfere with the radiation pattern of the patch. To maximize radiation from the patch, a thick, low dielectric constant material is often used for the bottom substrate, and a thin, high dielectric constant material is typically used for the top substrate. The most prominent aspect of this feed arrangement is its increased bandwidth, which is mostly due to an increase in the thickness of the microstrip patch antenna that is included in the design. This technique allows for the selection of a different substrate for the patch and the feed line, allowing for the achievement of optimal performance in both cases. The most significant disadvantage of this technology is the difficulty in fabrication due to the various layers that must be aligned properly.

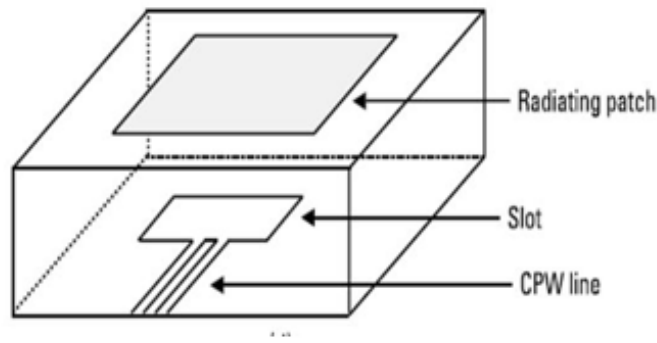


Figure 1.6: Microstrip Antenna fed by Proximity Coupled Microstrip Feed

1.6.5 Coplanar Wave Guide Feeding

Also discovered was that the coplanar waveguide feed may be used to excite the Microstrip antenna, which was previously unknown. The coplanar waveguide is printed on the ground surface of the patch to produce the desired outcome as illustrated in Figure 1.7. It is powered by a coaxial feed and terminated by a slot that is roughly one-quarter the length of the slot wavelength. A variety of features, including its wide bandwidth, simple structure, a single metallic layer, reduced number of soldering sites, and simplicity of integration with other circuits, have made it a popular choice in wireless communication systems. Because of the longer slot, this approach has a significant radiation dose, which is its primary drawback. Increasing the size of the slot and modifying its design to resemble a loop can make this situation better.

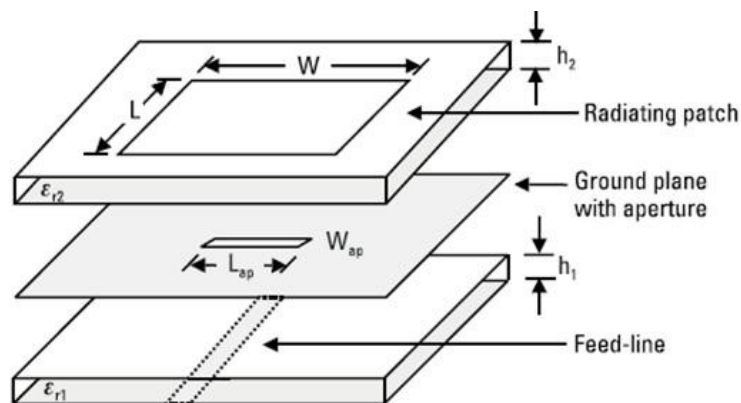


Figure 1.7: Microstrip Antenna fed by Coplanar Wave Guide Feed

1.7 Research Objectives

Based on the literature survey and gap analysis, it was observed that very little work has been done for detection and prevention of infiltration on the coastline of the country on the large scale or scalable for extensive needs. At present, most of the measures to detect and prevent coastal line activities are done by persons of coast guard and border security forces. However, continuous stream recorder (CSR sensor) is used to detect an intrusion of tiny boats with a length of fewer than 20 meters, and for any subversive operations taking place through the use of these tiny boats. The major concern with these sensors is coastal environment that has a significant impact on sensor performance and mechanical design.

The gap analysis motivate us to design the microwave sensors for coastal surveillance which is more robust and sustainable under uncertain coastal environment. With this objective, it is thought of to design the microstrip patch array antenna as a sensor in the allotted frequency band (x-band). The major requirements to design the antenna as a sensor for this application are narrow beam width and high gain. A wide range of microstrip antennas have been extensively researched for the customized applications. Although they have enticing features such as low profile, low cost, and ease of fabrication, but their poor power handling capability and high losses typically make them unsuitable for coastal monitoring applications. The material of the substrate is playing key role to control the gain and beam width of radiation. Therefore, to reduce the dielectric losses and to increase the gain and mechanical strength, following objectives are framed.

The objective of the research is as follows:

1. Design and fabrication of substrate with suitable dielectric properties.
2. Design and simulation of a Microstrip antenna array (operating in the X band) based on the proposed dielectric substrate.
3. Fabrication and Validation of the optimized Antenna array.

4. Validation of proposed concept through field testing.

Chapter 2

Literature Review

Since the advent of wireless communication technologies, the microstrip patch antenna has emerged as one of the most widely utilized antenna types available. Because of the huge number of applications and developments in communication systems nowadays, a small size antenna with increased bandwidth is necessary. Scientists have been experimenting with the properties of substrate materials and proper design in recent years.

2.1 Literature Survey

A significant deal of research has recently been focused on the qualities of survey of literature reviews and some of them are presented below.

Kapil Saraswat and Ayyangar R. Harish investigated a dual-band circularly polarized coplanar waveguide fed split-ring resonator-loaded rectangular slot antenna supplied by a coplanar waveguide [14]. By adjusting the size of the resonator, it is possible to produce a wide-frequency ratio that ranges from 1.2 to 2. An antenna with two bands, the first at 2.4 GHz and the second at 3.5 GHz, is developed and measured. The measured characteristics are compared with the simulation results, and it is discovered that they are in excellent agreement with each other. Following the obtained results, the proposed antenna is capable of operating on two frequency

bands with bandwidths ranging from 32.13 percent (2.22–3.07 GHz) to 2.17 percent (3.415–3.49 GHz).

Krishnamoorthy Kandasamy suggested a dual-band microstrip line fed antenna based on split-ring resonators, which was implemented in a microstrip line [15]. SRRs are put on the backside of the antenna slot to create the upper band that is circularly polarized. The corners of the slot that are diagonally opposite each other are shortened, which, in conjunction with the SRRs, produces Circular Polarization (CP) response in the bottom band. Due to the design flexibility of this dual-band antenna, it is possible to manage the resonance frequency and sense of polarization at each of the dual-bands independently. This antenna, which is meant to operate at frequencies of 3.1 GHz and 4.7 GHz, has been constructed and tested. In the lower and upper bands, the 3 dB axial ratio bandwidth is 3.1 percent (from 3.05 GHz to 3.15 GHz) and 4.2 percent (from 4.65 GHz to 4.85 GHz) in the lower and upper bands, respectively. A metallic cavity is utilized in conjunction with the antenna to produce a unidirectional radiation pattern with a front-to-back ratio of more than 15 dB while maintaining the impedance bandwidth at the same time.

Taiwei Yue constructed a small dual-band antenna with operational bands centered at 1.9 GHz and 2.5 GHz that was confirmed numerically as well as empirically and published their findings in *IEEE Transactions on Communications* [16]. This antenna is constructed by layering a monopole feeding antenna on top of an engineered multilayer met surface (MS), which serves as an artificial ground plane for the antenna transmission. Additional CSRR structures are included in the multilayer MS design to enable the monopole-MS integrated antenna system to operate in both the 2.4 GHz and 5.8 GHz frequencies. When the dispersive analysis of the MS unit cell is performed, the underlying radiation mechanism of the antenna is revealed. The designed MS functions in both frequency bands at the same time.

Farhad Farzami and colleagues discussed the downsizing of a rectangular mi-

crostrip antenna using a magneto-dielectric substrate both theoretically and practically in 2011 [17]. With the use of a metamaterial arrangement, it is possible to reduce the antenna dimensions by raising the constitutive parameters of the magneto-dielectric substrate, which is what is being sought. The predicted structure is also tiny enough to be incorporated into a certain dielectric substrate. When compared to a standard dielectric microstrip antenna, the suggested magneto-dielectric substrate at 2.4 GHz reduces the region of the microstrip antenna by up to 65 percent, resulting in a smaller overall footprint. However, because of the increase in magnetic permeability at the anticipated 2.4-GHz frequency, the bandwidth of the downsized antenna is almost completely unaffected by this increase. Finally, a tiny antenna that has been constructed is tested and measured. Approximately a linear relationship exists between measured and simulated findings.

Hassan Mirzaei investigated an accumulation frequency reconfigurability to a small metamaterial-inspired antenna, which was published in IEEE transaction [18]. With an integrated slot, this printed-monopole antenna receives its power from a coaxial power line (CPW). This antenna was first conceived as a result of the concept of negative-refractive-index metamaterial transmission lines, which have been shown to exhibit dual-band performance. Because of the employment of a varactor diode, it is possible to adjust the narrowband of the antenna, which is caused by radiation from the included slot, over a wide frequency range, while the higher band remains essentially constant. For the lower band of the antenna's frequency adjustment characteristics, a whole equivalent circuit model is built and used to estimate the characteristics of the antenna's frequency adjustment. It is explained by the investigational results that, for a varactor diode with capacitance values approximately ranging from 0.1–0.7 pF, tuning frequencies in the range of 1.6–2.23 GHz can be reached.

Cristhianne de Fátima Linhares de Vasconcelos discovered propagation characteristics ARMSA on metamaterial substrate using spectral-domain analysis, which

they published in IEEE transaction [19]. Through the use of Hertz vector expression, it is possible to obtain Green's functions of the structure in the Hankel transform domain. It is possible to acquire numerical results for resonance frequencies and return losses that are functions of the met material properties as well as a few geometrical parameters.

The metamaterial unit cell with a modest refractive index over a wide frequency band was conceived and designed by Dongying Li and colleagues. Obtaining the unit cell's valuable material parameters is accomplished, and the unit cell then goes on to produce a three-layer metamaterial structure that is used as a superstrate for broadside gain increase in a patch antenna operating at a frequency of 10 GHz [20]. The proposed superstrate is optimized in conjunction with the antenna to improve its beam-focusing performance while taking into consideration the oblique wave incidence from the radiation source. Using the improved superstrate, both simulation and measurement of the antenna have shown that this configuration is capable of achieving a broadside gain of 70 to 80 percent of the maximum gain possible from the ideal efficient radiating surface.

A small-size metamaterial-inspired antenna with increased bandwidth was developed by M. S. Majedi and colleagues [21]. For the fabrication of small antennas, metamaterial structures are frequently employed. Although many of these antennas have a narrow bandwidth, this is not the case for all. The suggested antenna is based on an epsilon-negative transmission line with a CPS construction, which serves as its inspiration. It is possible to reduce the size of the antenna by utilizing an ENG TL and operating at the ZOR frequency of the device. The use of a CPS-like structure improves the bandwidth of the antenna as well. According to the results of the measurements, the suggested antenna has an impedance bandwidth of 12.4 % at -10 dB.

Seung-Tae Ko and Jeong-Hae Lee suggested a hybrid zeroth-order resonance

patch antenna with a wide E-plane beamwidth along with a wide E-plane beamwidth [22]. It is necessary to combine the TM mode with the ZOR mode to obtain a large beam width from an antenna. It is simple to regulate the E-plane beamwidth of a TM mode by separating the incident power into two modes and dividing the incident power into two modes. TM mode and ZOR mode are produced simultaneously by inserting a mushroom antenna within a rectangular patch antenna that has been cut with an etched rectangular hole, and a single feed is used between two radiators to generate the two modes. With the aid of a feed, it is possible to adjust the incident power to each antenna separately. It is also discovered that both the antenna's bandwidth and its efficiency are 3.3 % and 92 %, respectively, of the total bandwidth. At long last, the measured data reveals that they are in excellent agreement with the simulated ones.

The researcher Li-Ming Si devised and constructed a novel small, planar, dual-band, and coplanar waveguide (CPW)-fed antenna with consideration given to the use of composite metamaterial [23]. A split-ring resonator (SRR) on the inside and a closed-ring resonator on the exterior is used in this type of metamaterial (CRR). CPW-fed lines with trapeziform ground planes and tapered impedance transformer lines are used to improve the impedance matching of the antenna by reducing the impedance mismatch. For the lower narrow frequency band, the inner SRR dimension is significantly less than the resonant wavelength, which allows the dual-band antenna to be exceedingly compact because it uses a much smaller inner SRR dimension than the resonant wavelength. The numerical simulation and experimental measurement of antenna parameters, as well as the reflection coefficient, are used to examine the results. There is a high degree of agreement between the simulation and the measurement.

Mishra and colleagues proposed Design and Analysis of Microstrip Patch Antenna for Wireless Communication [24]. The design analysis of rectangular and square shaped microstrip antennas is presented in this study. For feeding purposes,

both antennas utilised a microstrip line. In comparison to rectangular microstrip antennas, square-shaped microstrip antennas provide a broader bandwidth and enough return loss. The small antenna is designed to work in the X band of frequencies. The proposed microstrip antenna is showing a wide bandwidth of 500 MHz with a high return loss of -24 dB. This high bandwidth provides its usefulness in many wideband utilities in X-band.

Rashmitha and colleague presented a microstrip patch antenna design for fixed Communications [25]. They construct and simulate a microstrip patch antenna for wireless communications in this paper. The antenna is made of FR4 material. The antenna's return loss, VSWR, gain, radiation pattern, and current distribution have all been examined. The collected results are checked to ensure that they meet the requirements and are discussed in relation to a variety of applications.

Leela and Siddaiah proposed 1×4 Rectangular Patch Array Operating at 10 GHz Using Corporate Feeding Technique [26]. Modern communication systems require a more compact design that is low in cost, light in weight, and performs well across a wide frequency spectrum. Above all requirements, the microstrip antenna is the ideal choice. The rectangular patch microstrip antenna is constructed to operate at a frequency of 10 GHz. The rectangular patch element is then used to create a 1×4 array for improved performance in several aspects including as gain, return loss, and VSWR. This antenna is intended for all X-band applications.

Mohamed and Hussein proposed High Gain Compact Microstrip Patch Antenna for X-Band Applications [27]. This work provides a Frequency Selective Surface (FSS) design for a microstrip patch antenna operating in the X-band at 10 GHz to improve gain and efficiency. The band-stop frequency selective surface (FSS) is employed at the antenna's operating frequency. The superstrate for the microstrip patch antenna is the FSS structure. This paper's main purpose is to design a small microstrip antenna module. As a result of the simulation, there is a great gain and

efficiency. The suggested antenna module is exceedingly small and has a high gain, making it suitable for use in X-band applications.

Kandasamy suggested a dual-band microstrip line fed antenna based on splitting resonators [28]. Due to the design flexibility of this dual-band antenna, it is possible to manage the resonance frequency and sense of polarization at each of the dual-bands independently. This antenna, which is meant to operate at frequencies of 3.1 GHz and 4.7 GHz, has been constructed and tested. In the lower and upper bands, the 3 dB axial ratio bandwidth is 3.1 percent (from 3.05 GHz to 3.15 GHz) and 4.2 percent (from 4.65 GHz to 4.85 GHz) in the lower and upper bands, respectively. A metallic cavity is utilized in conjunction with the antenna to produce a unidirectional radiation pattern with a front-to-back ratio of more than 15 dB while maintaining the impedance bandwidth at the same time. This feature is good when maximum power to be focused on the narrow beam, and security features to be enhanced by dynamic polarisation.

Farzami and colleagues discussed the downsizing of a rectangular microstrip antenna using a magneto-dielectric substrate both theoretically and practically in 2011 [29]. With the use of a metamaterial arrangement, it is possible to reduce the antenna dimensions by raising the constitutive parameters of the magneto-dielectric substrate, which is what is being sought. The predicted structure is also tiny enough to be incorporated into a certain dielectric substrate. Finally, the antenna that has been constructed is tested and measured. Approximately a linear relationship exists between measured and simulated findings. This substrate with metamaterial arrangement becomes useful for improving the area of the patch antenna, but gain and beamwidth becomes poor.

Mirzaei investigated an accumulation frequency configurability to a small metamaterial-inspired antenna [30]. With an integrated slot, this printed-monopole antenna receives its power from a coaxial power line. This antenna was first conceived as a

result of the concept of negative-refractive-index metamaterial transmission lines, which have been shown to exhibit dual-band performance. It is demonstrated in the circuit model that the antenna operates in both even and odd modes during its operation. This arrangement becomes useful especially with a wider band and with encryptions to be implemented at sites where high interferences are present.

A small-size metamaterial-inspired antenna with increased bandwidth was developed by M. S. Majedi and colleagues [31]. The size of an antenna matters where patch array matrix is larger and high gain with lower bandwidth is needed. For the fabrication of small antennas, metamaterial structures are frequently employed. Although many of these antennas have a narrow bandwidth, which is very much important for coastal area surveillance. The use of a cyber physical system like structure improves the bandwidth of the antenna as well. According to the results of the measurements, the suggested antenna has an impedance bandwidth of 12.4/at -10 dB. This feature is attractive when we need narrow beamwidth is required.

Prathaban Mookiah discovered that a metamaterial with increased magnetic permeability can also improve the antenna array of a multiple-input multiple-output (MIMO) communication system [32]. Analyzed was the performance of a rectangular patch antenna array on top of a metamaterial substrate in comparison to the performance of the same array constructed on an ordinary FR4 substrate. Performance indicators such as array correlation coefficients and mean effective gain was used to compare the performance of widely dispersed arrays analytically. Results demonstrate that arrays on top of conventional FR4 substrates have high capacity due to gain and efficiency factors; however, when using a metamaterial substrate, arrays can be prepared smaller and have lower mutual coupling and correlation coefficients. So when antenna shrinking is a key design objective, metamaterial substrates are a more lucrative alternative than traditional substrates since they may achieve the same miniaturization factor without significantly compromising performance.

Ko and Lee suggested a hybrid zeroth-order resonance patch antenna with a wide E-plane beamwidth along with a wide E-plane beamwidth [33]. It is necessary to combine the Transverse Magnetic Modes mode to obtain a large beam width from an antenna. This feature is very relevant and useful in the transmission link between the sensors/ antenna is to be made code oriented rather than plan carrier wave to detect the intruder on the coastal line.

The stimulation of complex modes in lossless and similar structures was studied by Rubaiyat Islam [34]. They clarify several concepts that have been discussed in the literature about the excitation of complex mode pairs. They demonstrate that it is possible to adjust the excitation amplitude of an individual mode in a pair of conjugate complex modes in a realistic manner. The theoretical justification for the assumption is that such modes in a complex pair must be aroused with equal amplitudes for them to exist. Microwave circuit simulators have been used to verify the assertions made in this paper.

Pai Yen Chen investigated sub-wavelength elliptical patch antennas that were partially loaded with magnetic metamaterials to improve their performance [35]. For starters, they develop a universal theory for homogeneously loaded sub-wavelength elliptical patch antennas, from which they derive a closed-form explanation for the modes that can be sustained by this design within the long-wavelength range of interest. Theoretical studies demonstrate that their resonant dimension can be squeezed to any arbitrarily small dimension in principle, provided that the properties of the loading metamaterial are properly tailored. The researchers then discussed several advantages provided by the elliptical shape.

Li-Ming Si devised and constructed a novel small, planar, dual-band, and coplanar waveguide [36]. A split-ring resonator (SRR) on the inside and a closed-ring resonator on the exterior is used in this type of metamaterial Coupled Ring Resonator(CRR). This feature is good when multiple carriers to be used to enhance the detectability on the coastal line intrusion detection capabilities.

Abdalla and team suggested suggested an ultra-compact filtering integrated antenna for GPS and LTE (at frequencies of 1.57GHz and 2.65GHz, respectively) application. Integration of dual composite right or left-handed antennas [37]. with a band stop filter is accomplished in one stage by the antenna design. This feature is especially useful when antennas are to be made robust against the noise and interferences'. Integrated dual composite right or left handed antenna with band stop filtration provides extra amplitude and phase stability performances. Phase improvement of a multi-resonance composite right or left-handed unit cell for multi-band antennas. When the antenna goes for the production and deployment, the filtrations and the compactness are very useful.

Hussein Attia and colleagues suggested that utilizing the cavity model of microstrip antennas in conjunction with the reciprocity theorem as well as the transmission line analogy, it is recommended to calculate the radiation field of a microstrip antenna loaded with a generalized superstrate [38]. Comparing the analytical formulation for the antenna's far-field to full-wave numerical approaches reveals that the analytical formulation is significantly faster. It just requires a fraction of the time required by full-wave analysis (around 2%). As a result, the recommended method can be used for a variety of design and optimization purposes. Both numerical and experimental findings are used to verify the method's effectiveness. Here a viable microstrip patch antenna operating in the band of the Universal Mobile Telecommunications System has been designed and tested using the analytical method that has been proposed.

Islam and colleagues presented a small antenna based on planar-patterned metamaterial structures that might be used for ultra-wideband applications [39]. On the triangle patch, this antenna is constructed from four metamaterial unit cells that display both negative permeability and negative permittivity at the same time, as well as three rectangular slots on the partial ground plane, all of which are connected

by a thin microstrip line. Because of the usage of planar-patterned metamaterial arrangements, it has a wide bandwidth ranging from 3.07 to 19.91 GHz.

Antennas and microwave devices that rely on the isotropic medium were described by John L. Volakis and colleagues [40]. This allowed us a limited amount of creative freedom during the design phase. Anisotropic media, on the other hand, introduce several additional degrees of freedom (at least three additional degrees of freedom for dielectrics and three additional degrees of freedom for magnetic materials), opening up a new direction in the design of radiofrequency (RF) communication devices and wireless systems. The design of miniature antenna elements using dispersion engineering is next demonstrated on small finite substrates, followed by a demonstration of their presentation on small finite substrates. The second section of this work is concerned with the concatenation of DBE and MPC antenna elements to realize minor measurement wideband arrays of minor measurement. Such arrays take advantage of the current sheet antenna (CSA) concept to achieve the highly desired goal of compact wideband metamaterial arrays.

When it comes to miniaturization and improved performance of antennas using metamaterials, Navdeep Singh explained simulated results in addition to experimental results [41]. It is one of the goals to create devices that are smaller in size and have higher performance than previously achieved results. Their research shows that antennas constructed entirely of metamaterials are more efficient than antennas constructed entirely of other materials. Under the right conditions, these materials can be used to manufacture Efficient, Enhanced, Miniaturized, Single band or Multiband Operating, and Beam Steerable Antennas that are efficient, enhanced, and miniaturized

G. Jang S. Kahng discussed a microstrip bandpass filter for the UHF 900 MHz band that has been significantly miniaturized and characteristics have been improved through the use of metamaterial zeroth-order resonator (ZOR) properties [42]. According to the authors' recommendations, the bandpass filter's resonators should

be realized by a one-cell ZOR, and the coupling between neighboring various ZORs should be controlled to achieve the primary goal of bandpass filtering in the form of a sequential coupling mechanism. Second, because of source-load coupling, it is advised that this MTM ZOR filter have transmission zeros (TZs) to provide better isolation from other wireless communication bands. A dispersion diagram and a three-dimensional electromagnetic simulation of the no-phase deviation electric field distribution over the ZOR are used to confirm the MTM features.

Hussein Attia and colleague looked at the reciprocity theorem in conjunction with the transmission line analogy, and they used the cavity model to develop an extremely quick analytical explanation for the radiation fields of microstrip antenna arrays enclosed with magneto-dielectric superstrates [43]. The inclusion of a broadside coupled split-ring resonator (SRR) in the superstrate is planned, and it will be located approximately one-tenth of a wavelength apart from a 4x1 microstrip patch array operating at 2.2 GHz in the final design. The anticipated analytical formulation and the full-wave numerical simulations are found to be in excellent agreement with one another. It is possible to achieve a gain increase of approximately 3.5 dB after covering the antenna array with the engineered magnetic superstrate.

Reported on passive electrically very small antennas with minute radiation resistance and bandwidth, which were designed by Hassan Mirzaei [44]. There is a new type of active antenna in which an active circuit producing a non-Foster impedance is embedded within a metamaterial motivated little antenna with a normal sizable radiation resistance, which is a variation on the active antenna. The development of a compact, broadband antenna that is well-coordinated and has the potential to achieve high efficiency is finally complete. The use of this technology eliminates the need for an active (or passive) step-up transformer to increase the radiation resistance of the system. This work demonstrates the possibility of exploiting non-Foster elements implanted in metamaterial-based antenna design.

A negative metamaterial (MNG) created by Haider R. Khaleel and colleagues is used for mutual coupling reduction among dual-band printed monopole antennas used in Multiple Input Multiple Output (MIMO) systems (MIMO) [45]. Using a dual-band MNG metamaterial with entirely negative effective permeability at the two resonant frequencies in any environment where the antennas are operating, it is proposed to achieve this goal. MNG is interspersed between the two printed monopoles to minimize the correlation between the two. To operate in the Wireless Local Area Network (WLAN) bands 2.45 GHz and 5.2 GHz, the printed monopole antennas were created to operate.

A metamaterial (MTM) branch-line coupler with microstrip RFID reader antenna was presented by Youn-Kwon Jung [46]. To design the proposed antenna, an FR-4 substrate with a relative permittivity of 4.66 and a thickness of 1.6 mm is used. The MTM coupler is intended to be used in conjunction with the precise closed-form formulas that have been provided. The dual-band circularly polarized RFID reader antenna, which has various transmitter and receiver ports, is connected to the metamaterial (MTM) branch-line coupler that has been built for this application.

Yuandan Dong presented an inquiry for tiny patch antennas with complementary split-ring resonators and reactive impedance surfaces [47]. This is accomplished by including the CSRR on the patch as a low-resonance frequency shunt LC resonator. Additionally, the RIS is implemented by utilizing two-dimensional metallic patches printed on a metal-grounded substrate. By altering the layout of the CSRRs, it will be possible to achieve multi-band functioning with a variety of polarization states. Six different antennas are developed and compared, as well as a circularly polarized antenna, to demonstrate their versatility in real-world scenarios.

A microstrip array with improved performance was proposed by Ming-Chun Tang and colleagues [48]. The authors proposed an ultra-low-loss and broadband electric

metamaterial electromagnetic the metamaterial slab is constructed by edge-coupled split-ring resonators that are periodically grounded (PGESRRs). Exceptional gains are achieved, including peak isolation of more than -50 dB, 15 % fractional bandwidth (-10 dB isolation), and almost lossless operation. The performance of a 7x3 microstrip array was simulated to investigate the effect of manipulating the metamaterial slab on the array's performance. The findings indicate that the metamaterial slab can improve the radiation properties of microstrip phased arrays, as well as widen the scanning limit and remove grating lobes.

Raoul O. Ouedraogo and colleagues published a methodology for producing very tiny patch antennas [49]. The technique makes use of CSRRs that are arranged horizontally between the patch and the ground plane. With careful optimization of the diameters of the split rings, it is possible to achieve sub-wavelength resonance of the patch antenna while maintaining a high-quality impedance match and radiation properties that are comparable to those of a standard patch antenna. During calculations and tests, it is demonstrated that a circular patch resonant at a frequency of 2.45 GHz may be miniaturized to an extremely high degree. Although downsizing is achieved through a drop in radiation efficiency and bandwidth, antenna performance remains excellent even when the patch size is reduced by a factor of one-eighth.

Xin Mi Yang and colleagues investigated the decrease of mutual coupling among narrowly separated antenna elements, which was a significant finding [50]. The use of wave-guided metamaterials is being considered as an efficient method of suppressing the mutual coupling among microstrip patch antennas. It is proposed and implemented using crossed-meander-line slits, which disclose magnetic resonances in addition to the band-gap property of the metamaterials under consideration. Incorporating wave-guided metamaterials between two H-plane linked rectangular patch antennas with an edge-to-edge space less than $\lambda/8$ has resulted in a roughly 6 dB reduction in mutual coupling over a 10-dB bandwidth, as demonstrated in this paper.

A microstrip patch antenna with “Pentagonal Rings” metamaterial cover was constructed and examined by Bimal Garg and team at a height of 3.2 millimeters from the ground plane [51]. The antenna is intended to operate at a frequency of 2.31 GHz. When compared to a rectangular microstrip patch antenna alone, the proposed metamaterial has a significant impact on lowering the return loss and increasing the directivity of the antenna. It is reasonable for requiring little bandwidth space and minimal return loss at 2.31GHz to design the antenna as proposed. The benefit of this work is that it allows us to create and simulate the proposed artificial structure with simultaneously negative permittivity and permeability.

The work of Zhenzhe Liu in 2013 presented a way for increasing the gain of microstrip antennas by modifying their design. Split-ring resonators (SRRs) are implanted in a low-temperature co-fired ceramic (LTCC) substrate that is integrated with a single patch antenna to form a compact nested tridimensional resonator [52]. The SRRs structure has an upper boundary measurement of only 0.13g, which is extremely small. It is believed that the SRRs provide a high-efficiency magnetic response as well as an increase in negative effective permeability and that they act as a metamaterial insulator for returning surface waves.

Seyed Mohammad Hashemi and team proposed the use of electrically charged compact chiral resonators in microstrip designs for the production of weakly radiating stop-band transmission lines to reduce the amount of radiation [53]. The advantage of this design is that the ground can be protected from being engraved as a result of it. Additionally, as compared to earlier implementations based on complementary split-ring resonators, the dimension of negative permittivity lines loaded with spin-orbital chiral particles can be reduced to a fraction of their original size. The performance of both negative permittivity and double-negative lines loaded with electrically connected resonators may be accurately explained by circuit models that have been adequately extracted from their parameters. This parameter

extraction technique is based on the comparison of the simulated transmission and reflection characteristics of the host line loaded with such resonators and the transmission and reflection characteristics obtained from the lumped-element equivalent circuit model of the host line loaded with such resonators.

Falguni Raval developed a microstrip patch antenna in which metamaterial features were applied at the ground plane, as well as obtaining the effect of a microstrip patch antenna with and without a metamaterial structure [54]. The piece is primarily composed of metamaterial, such as a defective ground plane. In this paper, we construct and simulate the unit cell of a split-ring resonator using a high-frequency structure simulator, and we also recover the effective permeability of the unit cell from its S parameters. It is possible to lower the overall size of the metamaterial patch antenna by 70 percent. The properties of the antenna, such as the Return Loss and Gain, were measured.

Mahmoud A. Abdalla and colleague suggested an ultra-compact filtering integrated antenna for GPS and LTE (at frequencies of 1.57GHz and 2.65GHz, respectively) application [55]. Integration of dual composite right or left-handed antennas with a band stop filter is accomplished in one stage by the antenna design. When compared to conventional antennas of similar dimensions, the suggested antenna is only 6.5 percent more efficient at the GPS band and 16.5 percent more efficient at the LTE band. The design methods for individual antennas, bandstop filters, and filtering integrated antennas are all discussed in length in this section. The suggested antenna design is compact design as well as has filtering capacity, and it is an excellent candidate for implanted antenna applications.

Mahmoud A. Abdalla and team suggested a nonlinear phase improvement of a multi-resonance composite right or left-handed unit cell for multi-band antennas [56]. Diverse antennas with nonlinear enhanced phases, capable of operating across five different frequency bands, have been developed. The proposed anten-

nas are compact, allowing for a size reduction of up to 60%. when compared to traditional patch antennas operating at the same frequencies as the ones proposed. To verify the acquired phase improvement, two distinct configurations of composite right-handed cells were compared to one another. The investigation of simulations and the discussion of experimental data are covered. There appears to be a reasonable match between the measured and simulated outcomes.

Wenquan Cao published a paper in which they described their inquiry into the applications of metamaterial-based antennas [57]. They include planar antennas that have a multi-band multi-function process, high gain properties, and better beam scanning abilities, among other characteristics.

M.M. Islam and colleagues presented a small antenna based on planar-patterned metamaterial structures that might be used for ultra-wideband applications [58]. On the triangle patch, this antenna is constructed from four metamaterial unit cells that display both negative permeability and negative permittivity at the same time, as well as three rectangular slots on the partial ground plane, all of which are connected by a thin microstrip line. Because of the usage of planar-patterned metamaterial arrangements, it has a wide bandwidth ranging from 3.07 to 19.91 GHz for VSWR 2. It also has a typical gain of 5.62 dBi with a crest of 8.57 dBi and a typical VSWR of 2. An excellent agreement between simulations and experiments is attained.

G.K. Pandey presented a small Ultra-wideband (UWB) high gain microstrip patch antenna with planar metamaterial structures, which was subsequently published [59]. To construct the antenna, two layers of metamaterial structure were etched into the core radiating patch and two crossed-shaped slots were etched into the ground plane, resulting in two layers of metamaterial structure. Antennas can be constructed from FR4 substrate, which is quite inexpensive. The antenna's bands ranges from 3-12GHz, with a typical gain of 4dBi and a peak gain of 5.8 dBi at 9.5 GHz. The results of the simulation show that the antenna has good radiation

properties for use in UWB applications, as demonstrated by the simulation.

R. Seviour and colleagues investigated the consequence of subjecting a metamaterial to comparatively high-power electromagnetic waves, both statistically and empirically [60]. They have demonstrated that when subjected to one watt of radio frequency, a metamaterial consisting of a split ring resonator on an FR4 substrate can suffer combustion. This is demonstrated by comparing the numerical simulations to the actual results, which reveals that numerical models may be utilized to precisely calculate the thermal activities of metamaterial when subjected to high-power radio frequency.

2.2 Chapter Summary

Lot of work has been done on patch antenna and patch antenna array designs. Least attention is given to optimised the substrate material and patch designs towards making Microwave sensors. No work has been reported in the literature to address the coastal security by using the microstrip antenna as a sensor. The gap identified here motivated us to synthesis the new substrate for making making a suitable sensor capable to operate in coastal environment.

Chapter 3

Design, Fabrication and Testing of Proposed Substrate SLTL-TB11

To achieve the goal of designing the “microwave sensor to detect the intrusion on the coastal line”, the most important component is dielectric substrate material. These sensors need to work in harsh outdoor environments in coastal areas. The sensor will consist of a substrate material, copper cladding/ lamination, and patch array with feed network.

Designing most appropriate substrates in microstrip based outdoor sensors is one of the key parameters to solve for the given ‘problem statement’. Along with the dielectric parameters, the sufficient flexibility and low moisture absorption coefficient are the key mechanical property needed for the Microwave sensors.

The overall cost of the system will be highly affected by dielectric material, hence it requires intelligent decision while designing the substrate material. Generally a dielectric substrate is defined by its two prime parameters besides few others as described earlier in this chapter. One is its permittivity, referred as ϵ (it describes the materials with high polarizability) and another is loss tangent, referred as $\tan\delta$ (it explains the dissipation of electromagnetic energy in the substrate). For the lossless materials there is no loss tangent ($\tan\delta=0$) the permittivity is real and therefore, $\epsilon = \epsilon_r \epsilon_0$.

3.1 Needs of customized Substrate material

The GAP analysis indicates that, based on the 6 parameters, ‘Dielectric constant’, ‘Loss tangent’, ‘Thermal coefficient’, ‘Dimensional stability’, ‘Tensile modulus’, and ‘Moisture absorption’, there is a need of customised substrate. This customised substrate is the desired dielectric coefficient from the limiting value of 13 to 15. The customised substrate also needs to have flexibility enhancement (tensile modulus) from 190 to 225 kpsi, The customised substrate is targeted to bring down the loss tangent to 0.0016, thermal coefficient to 15ppm/Degree Celsius, dimensional stability around 0.2mm/ meter or better, tensile modulus close to 180 kpsi and moisture absorption as close as 0,015% to suit the harsh and outdoor environment of coastal line microwave sensor operated at pulse power of 1000 watts.

Several materials were studied, and three materials were chosen for fabricating prototypes. Out of these three, two substrates were selected from commercially available material, namely FR4 and RO3006, whereas one was designed with optimum specifications to solve the given problem statement.

3.1.1 FR4

FR-4 is a glass-reinforced epoxy laminate material that is used in making PCBs and Patch antennas upto lower microwave bands or 2GHz. FR-4 is a flame-resistant composite material made of woven fiberglass fabric and an epoxy resin binder [61]. "FR" is an abbreviation for flame retardant, and it does not imply that a material conforms with the UL94V-0 standard unless it has been tested by UL 94, Vertical Flame testing in Section 8 at a compliant laboratory. The National Electrical Manufacturers Association (NEMA) established the designation FR-4 in 1968. FR-4 glass epoxy is a popular and adaptable high-pressure thermoset plastic laminate grade with excellent strength-to-weight ratios that are used in a variety of applications. Because of its low water absorption, FR-4 is most typically employed as an electrical insulator because of its high mechanical strength and low water absorption. When exposed to both dry and humid circumstances, the material is noted for

maintaining its strong mechanical values and electrical insulating properties. Due to these qualities, as well as the fact that it has superior fabrication characteristics, this grade is suitable for a wide range of electrical and mechanical applications [62]. Glass epoxy laminates are classified into the following grades: G-10, G-11, FR-4, FR-5, and FR-6. FR-4 is the grade that is currently most extensively used among these materials. However, G-10, which was developed before FR-4, does not possess the self-extinguishing flammability features of FR-4. As a result, FR-4 has largely replaced G-10 in most applications. The use of bromine, a halogen compound, in FR-4 epoxy resin systems is common to improve the flame-resistant qualities of FR-4 glass epoxy laminates.

3.1.2 Roger RO3000

For higher frequencies beyond 2 GHz, the most popular material is from Rogers® Corporation, USA is a nearly 2 century old company having quite a good range of monopoly microwave materials. RO3000® high-frequency circuit materials are ceramic-filled PTFE composites designed for use in the commercial microwave and RF applications. RO3000 high-frequency circuit materials are available in a variety of configurations. This line of products was created to provide superior electrical and mechanical stability at low prices while maintaining high-quality standards. Laminated circuit materials of the RO3000® series are made of ceramic-filled PTFE and have mechanical qualities that are consistent regardless of the dielectric constant used [63]. This was an easy decision to benchmark the customised substrate with RO3000® materials. When measured in the X and Y axes, RO3000 materials display a coefficient of thermal expansion (CTE) of 17 parts per million per degree Celsius. Its expansion coefficient is identical to that of copper, resulting in exceptional dimensional stability, with typical etch shrinkage (after etch and bake) of less than 0.5 miles per inch. The CTE along the Z-axis is 24 ppm/°C, which results in remarkable plated through-hole reliability, even in the most extreme thermal conditions. The relationship between the dielectric constant and temperature

for RO3035^(TM) materials is extremely stable.

For good radiation efficiency, general microstrip patch antennas at microwave frequencies use substrates such as quartz, PTFE, and honeycomb [64]. The electrical performance of these materials is pretty good, but the expense of using them for commercial applications such as mobile communication, direct broadcasting satellite reception, and so on is extremely high. In general, the cost of printed antennas is determined solely by the substrate material and connectors. FR4 is a low-cost material that is commercially available for printed antennas above 1 GHz but exhibit the low gain. Moreover, Flexible electronics is important in a variety of industries, including telecommunications, automotive, medical, and aerospace. As a result, there is a growing demand for flexible circuits. Therefore, substrate makers introduced a plethora of materials with high electrical performance along with flexibility at a low cost.

3.2 New Dielectric Substrate Material Composition STTL-TB11

There is two important material used in the proposed substrate Butyl Rubber and Titanium Dioxide.

3.2.1 Butyl Rubber

Butyl rubber is a synthetic rubber that is commonly used in applications requiring an air tight seal, such as roofing. It is also available in natural rubber. The combination of excellent weathering capabilities with low gas and moisture permeability is one of the most important attributes. Butyl rubber exhibits excellent resistance to ozone, ultraviolet light, as well as extremes of high and low temperature. Moreover, it possesses exceptional rip and bends resistance as well as stress and impact resistance. It is also resistant to heat aging and chemical attack. However, they have

a very low relative permittivity (ϵ_r) of the order of 2, making them unsuitable for use as the core of a flexible waveguide. They also have low heat conductivity and a high coefficient of thermal expansion, both of which are undesirable for substrate applications. Ceramics, on the other hand, are widely recognised for their high (ϵ_r) value, high heat conductivity, and limited thermal expansion [65]. They are, nevertheless, extremely brittle. As a result, neither elastomers nor ceramics may be employed in applications that need flexibility as well as high relative permittivity. All of the superior properties of the ingredients are present in the elastomer-ceramic composites.

Young modulus of Butyl (substrate) and Aluminium (housing and backplane support) shows that the microwave sensors made up of Butyl rubber based substrate will not go into fatigue as aluminium deforms due to temperature, vibrations as well as impacts on the outdoor costalline situations. The mechanical testing of butyl rubber is carried out and measured strain-stress characteristics are listed in Table 3.1.

	Stress at t=0 s (MPA)	Stress at t=7000 s (MPA)
50% strain	0.25	0.18
20% strain	0.137	0.098
Ratio of stress	1.83	1.84

Table 3.1: strain-stress characteristics of Butyl rubber

3.2.2 Titanium dioxide (TiO₂)

Titanium dioxide (TiO₂), also known as titanium oxide or titania, is a naturally occurring oxide of titanium. The mesoporous TiO₂ material is one of the most actively explored mesoporous materials because of their huge surface area and inherent porosity and wide range of potential applications. Mesoporous TiO₂ materials can be categorized into two types based on the arrangement of pores in space: those with a disordered structure, and those with an ordered structure [66]. Because of the accumulation of particles on top of each other, the pores formed by the accumulation

between particles in disordered mesoporous TiO₂ are irregular and not interconnected; on the other hand, in ordered mesoporous materials, the pores are regularly arranged in space, and the pore size distribution is narrow. Making mesoporous TiO₂ normally entails creating mesoporous gaps (2–50 nm in size) and arranging them in constructed arrays, which is a time-consuming process. Sol-gel synthesis, hydrothermal and solvothermal synthesis and template synthesis are some of the most extensively utilized synthesis processes [67]. Variable synthesis processes result in mesoporous TiO₂ materials with varying morphologies, mesostructures, pore diameters, doping, and crystallization, as well as different pore sizes. These properties are crucial for applications since they are structurally important. The microwave, physical and thermal properties of TiO₂ are listed Table-3.1

Property	Value
Chemical formula	TiO ₂
Molar mass	79.866 g/mol
Appearance	White solid
Odor	Odorless
Density	4.23 g/cm ³ (<i>rutile</i>), 3.78g/cm ³ (<i>anatase</i>)
Melting point	1,843 °C
Boiling point	2,972 °C
Solubility in water	Insoluble
Band gap	3.05 eV (rutile)
Magnetic susceptibility	5.9×10^{-6} cm ³ /mol
Refractive index	2.609 (rutile), 2.488 (anatase)

Table 3.2: Microwave, physical and thermal properties of TiO₂ [84,85]

3.2.3 Butyl Rubber-SrTiO₃

The potential of composite materials for electrical applications has already been demonstrated, and a significant number of articles on polymer–ceramic dielectric composites are accessible. Only a small number of researchers, however, are devoted to the development of mechanically flexible dielectrics for microwave applications.

Hakim and his team published a paper on the microwave dielectric characteristics of butyl rubber mixes that contained talc, calcium carbonate, barytes, dolomite, kaolin, and precipitated silica, amongst other ingredients [68]. Although they developed composites with very modest filler loadings (30 and 50 weight percent), they were unable to significantly improve the dielectric characteristics of the materials. Butyl rubber (BR) is used as the matrix and SrTiO₃ (ST) powder is used as the filler in this formulation [69]. In addition to being highly flexible, butyl rubber has low dielectric loss and high relative permeability as well as superior weathering resilience, which are all advantages of utilizing butyl rubber. At microwave frequencies, the relative permittivity (ϵ_r) of butyl rubber is approximately 2.4, while the dielectric loss tangent ($\tan\delta$) is on the order of 10^{-3} . The Butyl Rubber-ST composite demonstrates the significantly high relative permittivity (ϵ_r)=11.8) and low loss tangent ($\tan\delta$ =0.0018) at 5 GHz [70].

3.3 The proposed Substrate SLTL TB-11

The synonym “SLTL” is ‘dedicated’ to M/S Sahajanand Laser Technology Limited (SLTL), who has supported the research and development of dielectric substrate for solving the ‘problem statement’ of designing the appropriate microwave substrate. New Dielectric Substrate Material Composition of STTL-TB-11 is highly optimized for the target application microwave sensors for coastline security. To design the composite substrate materials, the process and the fabrication technique are elaborate in this chapter.

There are no established vendors or process houses having ‘process knowledge’ or identified infrastructure to get the targeted material TB-11. With interactive experimentations and testing, the fabrication process has been established.

The flow chart of the fabrication process has reported in Figure 3.1. The butyl is churned heavily to get the homogeneous paste. The paste is rolled uniformly to prepare a sheet of desired thickness of 1.5mm. The titanium oxide is sprayed over the surface with around 20 micron thickness. The sheets are cured in the ‘thermal-

vacuum' chamber to get the required substrate.

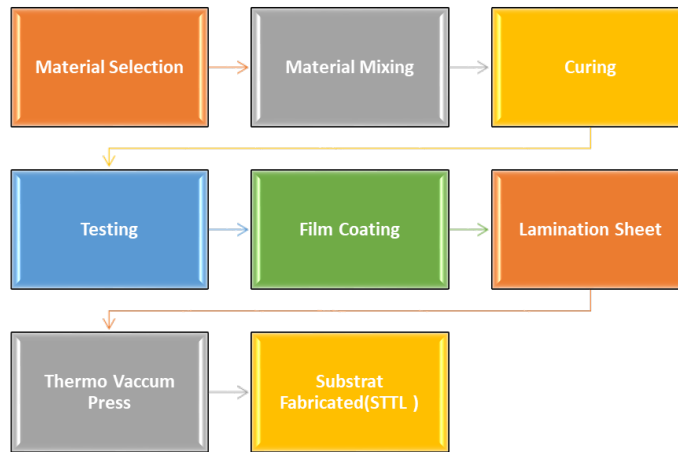


Figure 3.1: Fabrication process of proposed substrate

3.4 Testing Method

The dielectric, thermal and mechanical properties of the composite material were studied as a function of frequency and the losses inside the substrate at x-band frequency region. The “Test methods” used to characterize substrate are described as under:

- ASTM D638 specifies methods for testing the tensile strength of plastics and other resin materials and for calculating their mechanical properties, and outlines accuracy requirements for the test frames and accessories used. This test method uses dumbbell-shaped specimens with either a 25 mm or 50 mm gauge length. To determine the suitability of a material for an application where it is under load, measuring its elongation is important. Measuring elongation enables determination of the elastic modulus (reversible elongation in the elastic region) by measuring the small initial elongation range, and determination of elongation at specimen failure, by measuring larger irreversible elongation in the plastic region. Shimadzu’s SIE-560A series automatic extensometers accomplish both of these measurements with high accuracy, and provide automated functions that increase testing efficiency and test reproducibility [71].

- Differential Phase Length Method is a transmission/reflection method which is typically less accurate than resonator methods. However the differential phase-length method provides dielectric constant values over a wide range of frequencies whereas the resonator methods typically yield dielectric constant results at one or more discrete frequencies.
- IPC-TM-650 test method is intended for the rapid measurement of the X-band (8.00 to 12.40 GHz) relative permittivity and loss tangent of metal clad substrates. Measurements are made under stripline conditions using a resonant element pattern card, which is separated from the ground planes by sheets of the material to be tested. Further information about this method may be found in ASTM D3380-75.
- IPC-TM-650 2.6.2 test method is used for determining the amount of water absorbed by substrate when immersed in distilled water for 24 hours.

Property	FR4	RO-3006	SLTL-TB11	Unit	Condition	Test Method
Tensile Modulus	630	290	189	Kpsi	23°C	ASTM D 638
Dielectric Constant	4.4	6.3	10.5		8 GHz to 12 GHz	Differential Phase Length Method
Moisture Absorption	0.1	0.02	0.017	%	D48/50	IPC-TM-650 2.6.2.1
Loss tangent	0.018	0.002	0.0016		10 GHz /23°C	IPC-TM-650 2.5.5.5
Thermal Coefficient	18	17	15	ppm /°C	10 GHz 0°-60°C	IPC-TM-650 2.5.5.5
Dimensional Stability	0.4	0.27	0.2	mm /m	COND A	IPC-TM-650 2.2.4

Table 3.3: Parametric comparison of FR4, RO3006 and Customised substrate TB-11

Table-3.1 describes the performance parameters of the SLTL-TB11 substrate. To demonstrate the superiority of the present substrate, its performance is compared with marketing competitors (FR4 and RO3006) at 10GHz. The comparison made in

Table 3.3 clearly shows the superior mechanical, thermal and dielectric performance of the SLTL-TB-11 substrate. The enhanced mechanical and thermal performance of proposed substrate is advocating its application in harsh outdoor environments like in coastal areas.

3.5 Chapter Summary

This chapter provides the details of material used and the process steps of synthesis of SLTL-TB11 substrate. it is note that the proposed substrate ha superior mechanical, thermal and dielectric properties in comparison to its marketing competitors (FR4 and RO3006). The substrate is found to be suitable in designing microstrip patch array antenna which will serve as as sensor for coastal surveillance. The enhanced dielectric performance (dielectric constant and loss tangent) will help in achieving the high gain and to control the beam width of microstrip patch array antenna as discussed in the chapter 4.

Chapter 4

Antenna Array Design Using Different Substrate

In this chapter, three patch antenna array with three different substrates have been investigated. The three substrate material are FR4(cheap and robust), RO3006 (very low loss tangent) and SLTL-TB11 (fabricated and explained in previous chapter). The all three proposed antenna designs were simulated on CST software and experimentally tested. The validation of final designed microstrip antenna is carried out by comparing the simulated results (S11 parameters, VSWR and gain) of all three proposed designs.

It is observed that the microstrip antenna with SLTL substrate having the better performance over other two antenna and suitable for coastal security application purposes. Therefore, third design with SBTL substrate is fabricated and the simulation and experimental results are compared to validate the final design.

4.1 Design Specifications

To be successful, the overall purpose of a design must satisfy established performance parameters in its operating frequency. The first step in making a microstrip antenna is determining the operating frequency and the optimum substrate material. The dielectric constant and loss tangent were taken into account when calculating the

substrate parameters.

The operating frequency for the application of coastal security is allocated in the x-band and taken as 10 GHz for this study.

4.1.1 Dimension of Patch Antenna

The rectangular patch antenna is considered as the simplest one, in which, the length and width of the antenna are the two most critical variables to take into consideration. The resonance frequency of the microstrip patch antenna is determined by its dimension.

The width of the patch is given as:

$$W = \frac{c}{2f} \times \sqrt{\frac{2}{(\epsilon_{r+1})}} \quad (4.1)$$

The length L of the patch is given as:

$$L = L_{eff} - 2\Delta L \quad (4.2)$$

Where, the effective length L_{eff} is given as:

$$L_{eff} = \frac{c}{2f\sqrt{\epsilon_{eff}}} \quad (4.3)$$

ϵ_{eff} is the effective permittivity of the substrate and is given as:

$$\epsilon_{eff} = \frac{\epsilon_r + 1}{2} + \frac{\epsilon_r - 1}{2} \sqrt{[1 + 12\frac{h}{W}]} \quad (4.4)$$

By considering the normalized extension, the actual length of patch L is given as:

$$L = \frac{c}{2f} \left(\frac{\epsilon_r + 1}{2} + \frac{\epsilon_r - 1}{2} \sqrt{[1 + 12\frac{h}{W}]} \right)^{-\frac{1}{2}} - 2\Delta L \quad (4.5)$$

4.1.2 Dimension of Substrate

The substrate of a patch antenna is the layer which binds the patch and the ground plane. The size of the substrate and the ground plane are same, and it is related to the width and length of the patch as per the following equations [2].

The width of the substrate is given as:

$$W_s = W + 6 \times h \quad (4.6)$$

The length L of the patch is given as:

$$L_s = L + 6 \times h \quad (4.7)$$

where h is the height of the substrate.

The structure of one antenna element is shown in Figure 4.1, whereas the proposed 8x1 array is shown in Figure 4.2.

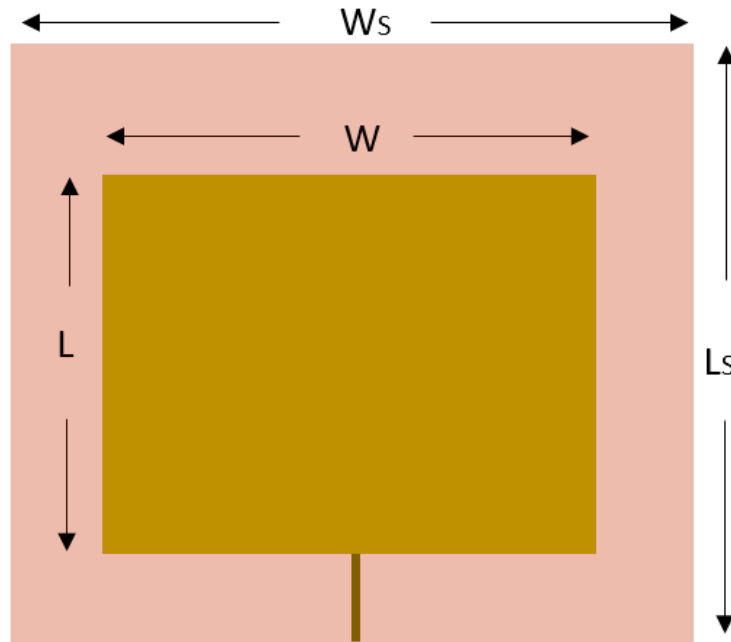


Figure 4.1: Schematic representation of One element of patch antenna

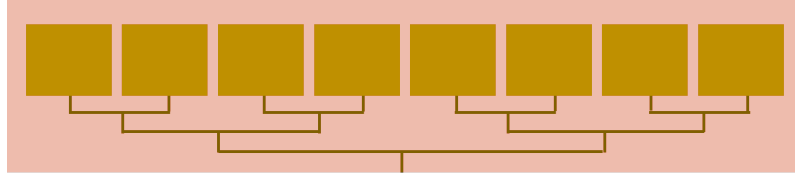


Figure 4.2: Schematic representation of 8x1 Antenna Array

4.2 Design of Microstrip Patch Antenna Array using FR4 substrate

In this section, the symmetrical 8x1 patch array is proposed on the FR4 substrate. The dimensional parameters of proposed design are optimized and reported in Table-4.1.

Parameters	Values (in mm)
Operating frequency	10 GHz
Dielectric Constant	4.4
Loss tangent	0.02
Width of patch element	9.1 mm
Length of patch element	7.8 mm
Width of strip-line connected to patch	0.15 mm
Length of strip-line connected to patch	2 mm

Table 4.1: Design Parameter of array antenna using FR4

4.2.1 Simulation Results and Discussion

The results in terms of S11 parameter, VSWR, and Gain obtained from the CST simulator for FR4 array antenna is discussed herewith.

4.2.1.1 S11 Parameter and Bandwidth

The observation for the variation of S11 parameter is recorded from 9 GHz to 11 GHz, as this range is the middle of the X-band. The FR4 antenna array shows a functioning from 9.5 GHz onwards. This antenna array has achieved a high value

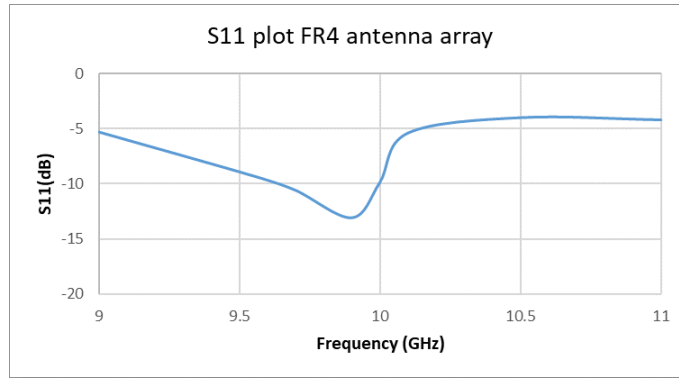


Figure 4.3: S11 parameter of FR4 for Microstrip feed Array.

of S11 of the magnitude -14.7 dB at 9.85 GHz of resonant frequency. The variation is shown in Figure 4.3. The bandwidth, on the scale of -10dB, is found to be 270 MHz. At this resonant frequency, the antenna radiates maximum power.

4.2.1.2 Voltage Standing Wave Ratio (VSWR)

VSWR is a measure of impedance matching of antenna with feedline. If the antenna radiates all of its transmitted power within the operating range of frequency then VSWR will be less than 2. The variation of VSWR of FR4 patch array antenna is shown in Figure 4.4. The magnitude of VSWR obtained is 1.44 at 9.854 GHz of resonant frequency.

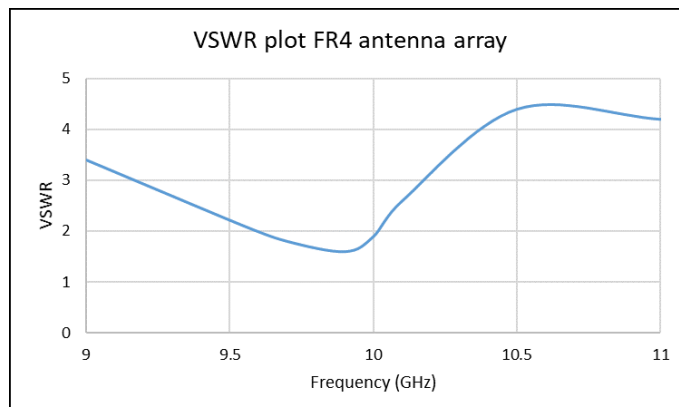


Figure 4.4: VSWR of FR4 Antenna Array

4.2.1.3 Gain

The gain of the antenna array design using FR4 is shown in Figure 4.5. The gain exhibits by the array is more than 9 dB in the frequency region ranging from 9.5 GHz to 10.1 GHz, and the gain achieved at the resonance frequency of 9.852 GHz is 11 dB. This array gives a very high gain throughout 9 GHz to 11 GHz of frequency.

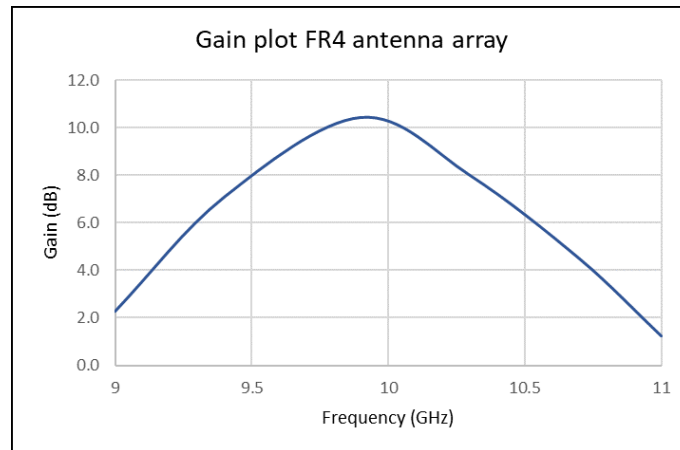


Figure 4.5: Gain of FR4 Antenna Array

4.2.1.4 Radiation pattern

Figure 4.6 shows the far-field radiation pattern of the FR4 array antenna. The radiation pattern of this array antenna is highly directional with little back lobes. The antenna achieved a beamwidth of 11.5 degree at 9.85 GHz of resonant frequency. The antenna pattern is highly directive and with high gain.

4.3 Design of Microstrip Patch Antenna Array using RO-3006

ROGERS-3006 (RO – 3006) is the substrate material of low dielectric constant, low loss tangent and it is engineered to meet the unique electrical, thermal, and mechanical requirements. The parameters for the second design of an array are shown

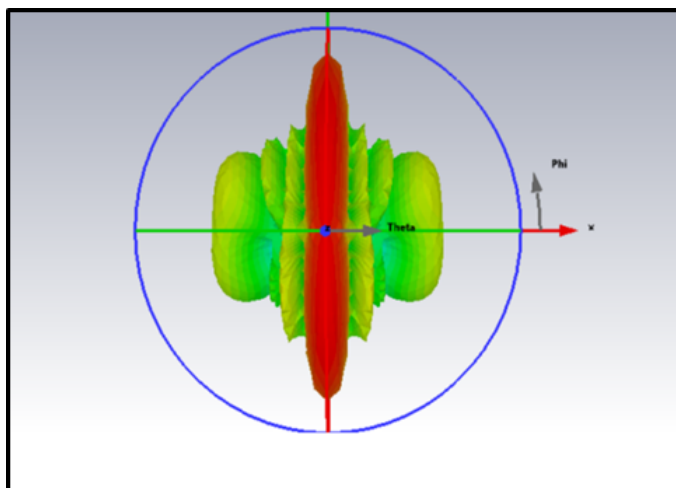


Figure 4.6: Radiation Pattern of FR4 Array Antenna

in Table 4.2, whereas Figure 4.6 shows the design array antenna using RO3006.

Parameters	Values (in mm)
Operating frequency	10 GHz
Dielectric Constant	6.3
Loss tangent	0.002
Width of patch element	7.8 mm
Length of patch element	6.6 mm
Width of strip-line connected to patch	0.15 mm
Length of strip-line connected to patch	2 mm

Table 4.2: Design Parameter of array antenna using RO3006

4.3.1 Simulation Results and Discussion

The results in terms of S11 parameter, VSWR, Gain and radiation pattern obtained from the analysis of RO3006 array antenna is discussed herewith.

4.3.1.1 S11 parameter and bandwidth

The observation for the variation of S11 parameter is recorded from 9 GHz to 11 GHz. The RO3006 antenna array shows a functioning from 9.5 GHz onwards. This antenna array has achieved a high value of S11 of the magnitude – 16.4 dB at 9.77

GHz of resonant frequency. The variation is shown in Figure 4.7. The bandwidth, on the scale of -10dB, is found to be 220 MHz. At this resonant frequency, the antenna radiates maximum power.

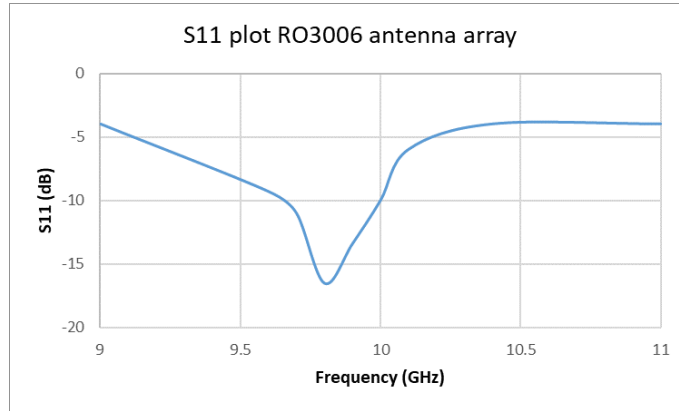


Figure 4.7: S11 parameter of RO3006 Antenna Array

4.3.1.2 Voltage Standing Wave Ratio (VSWR)

VSWR is a measure of impedance matching of antenna with feedline. If the antenna radiates all of its transmitted power within the operating range of frequency then VSWR will be less than 2. The variation of VSWR of RO3006 array antenna is shown in Figure 4.8. The magnitude of VSWR obtained is 1.35 at 9.77 GHz of resonant frequency.

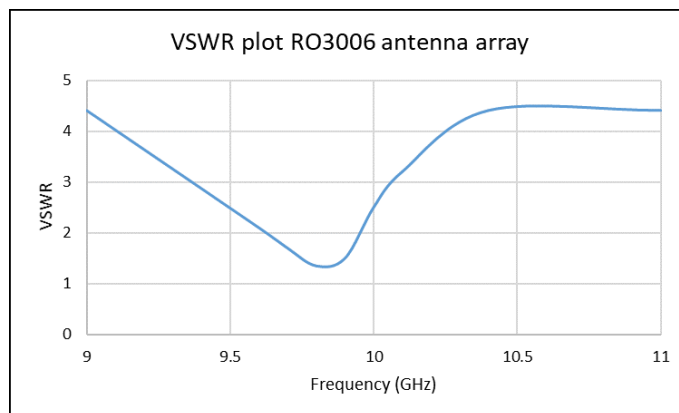


Figure 4.8: VSWR of of RO3006 Antenna Array

4.3.1.3 Gain

The gain of the antenna array design using RO3006 is shown in Figure 4.9. The total gain exhibits by the array is more than 6 dB in the frequency region ranging from 9 GHz to 10.2 GHz, and the gain achieved at the resonance frequency of 9.774 GHz is 12.5 dB. This array gives a very high gain throughout 9 GHz to 11 GHz of frequency.

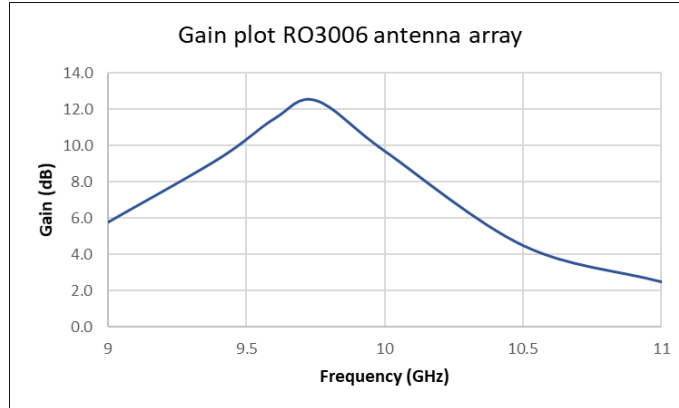


Figure 4.9: Gain of RO3006 Antenna Array

4.3.1.4 Radiation pattern

The radiation pattern of the RO3006 array antenna is shown in Figure 4.10. The radiation pattern of this array antenna is highly directional with little back lobes. The antenna achieved a beamwidth of 10 degree at 9.77 GHz of resonant frequency. The antenna pattern is highly directive and with high gain.

4.4 Design of Microstrip Patch Antenna using Substrate SLTL-TB11

In this section, the 8x1 patch array is simulated with SLTL-TB11 substrate. the dimensional parameters of proposed design are optimized and reported in Table 4.3.

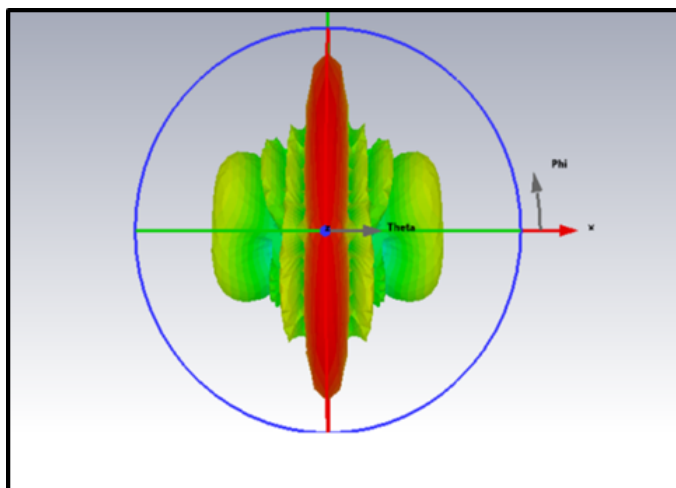


Figure 4.10: Radiation pattern of RO3006 Antenna Array

Parameters	Values (in mm)
Operating frequency	10 GHz
Dielectric Constant	10.97
Loss tangent	0.0016
Width of patch element	6.1 mm
Length of patch element	5.1 mm
Width of strip-line connected to patch	0.15 mm
Length of strip-line connected to patch	2 mm

Table 4.3: Design Parameter of Antenna Array using SLTL-TB11

4.4.1 Simulation Results and Discussion

The results in terms of S11 parameter, VSWR, Gain and radiation pattern obtained simulation from the analysis of STBL array antenna is discussed herewith.

4.4.1.1 S11 Parameter and Bandwidth

The observation for the variation of S11 parameter is recorded from 9 GHz to 11 GHz, as this range is the middle of the X-band. The proposed antenna array using SLTL-TB11 substrate radiating from 9.5 GHz onward. This antenna array has achieved a high value of S11 of the magnitude -19.3 dB at precisely 10 GHz of resonant frequency. The variation is shown in Figure 4.11. The bandwidth, on the scale of -10dB, is found to be 110 MHz, making it a high pointed one. At this resonant frequency, the antenna radiates maximum power.

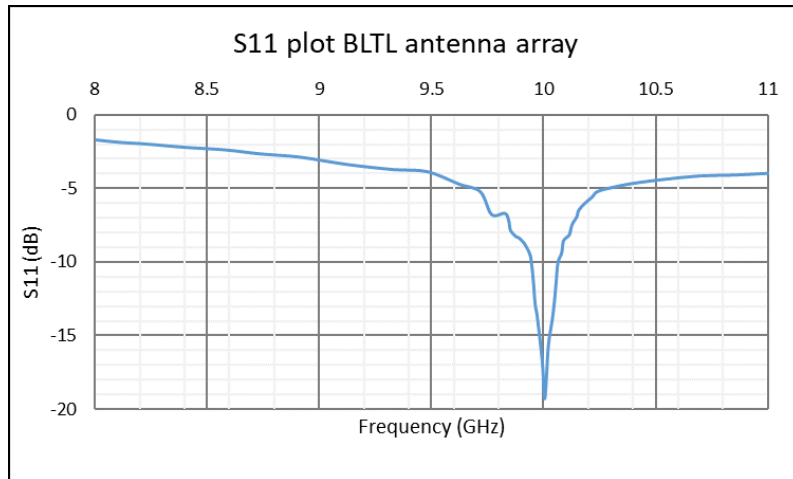


Figure 4.11: S11 of Antenna Array using SLTL-TB11

4.4.1.2 Voltage Standing Wave Ratio (VSWR)

VSWR is a measure of impedance matching of antenna with feedline. If the antenna radiates all of its transmitted power within the operating range of frequency then VSWR will be less than 2. The variation of VSWR of FR4 patch array antenna is shown in Figure 4.12. The magnitude of VSWR obtained is 1.24 at 10.015 GHz of resonant frequency.

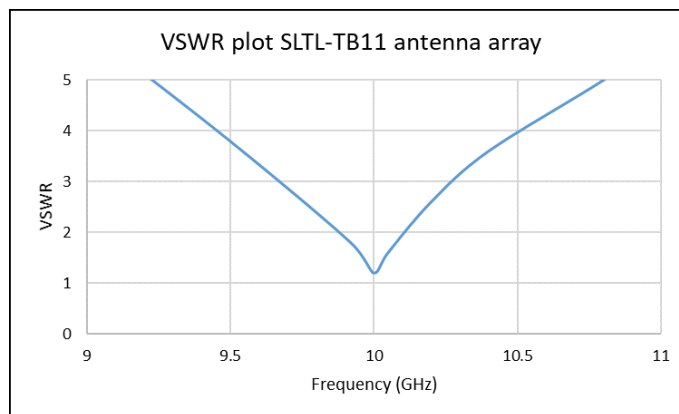


Figure 4.12: VSWR of Antenna Array using SLTL-TB11

4.4.1.3 Gain

The gain of the antenna array design using SLTL is very high and sharp as shown in Figure 4.13. The total gain exhibits by the array is 14 dB at 10 GHz of frequency. This proposed array provies a high gain at precisely 10 GHz of the desired frequency.

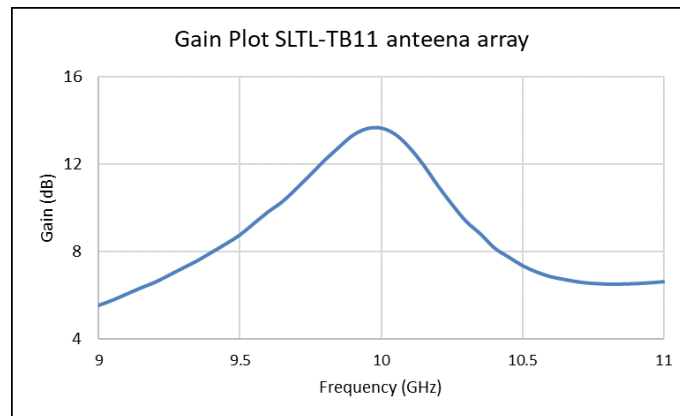


Figure 4.13: Gain of Antenna Array using SLTL-TB11

4.4.1.4 Radiation pattern

The far-field radiation pattern with SLTL array antenna is shown in Figure 4.14. The radiation pattern of this array antenna is also highly directional with little back lobes. The antenna achieved a narrow beamwidth of 7 degree at 10 GHz of resonant frequency. The high directivity coupled with high gain makes it a perfect choice for any imaging purposes.

4.5 Comparison of Antenna array results obtained three substrate

The comparison is made to compare the performance of all three designed antenn aaray and reported in Table 4.4

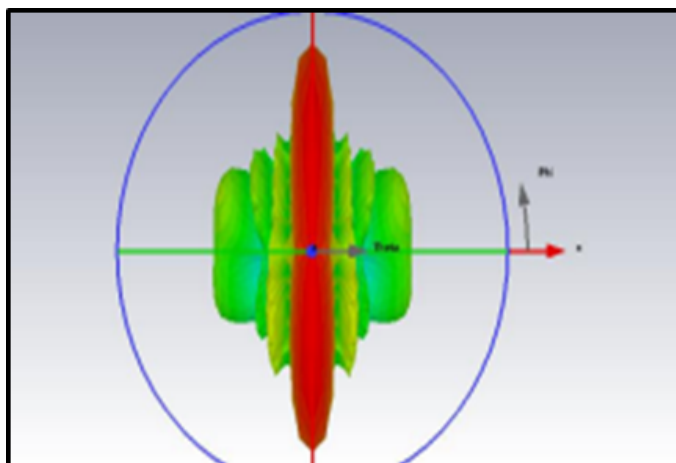


Figure 4.14: Radiation pattern Antenna array using SLTL-TB11

Substrate Material	Resonant frequency	S11	VSWR	Gain	Beamwidth
FR4	9.875 GHz	-14.7 dB	1.44	11 dB	11.5 degree
RO3006	9.774 GHz	-16.4 dB	1.35	12.5 dB	10 degree
SLTL-TB11	10.01 GHz	-19.3 dB	1.24	14 dB	7 degree

Table 4.4: Result characteristics of the antenna array using three substrates

The comparative analysis reveals that the microstrip antenna with SLTL-TB11 substrate outperforms in terms of gain and beamwidth than the other two antennas and it makes suitable for coastal security applications. Finally, the array antenna with SLTL-TB11 substrate is chosen for testing purpose, since it possesses high gain and low beamwidth as reflected in Figure 4.15.

4.6 Fabrication of Antenna Array using SLTL-TB11 substrate

The post validation of the design is done by the actual hardware fabrication.

The hardware of the antenna array is fabricated by means of computer Controlled

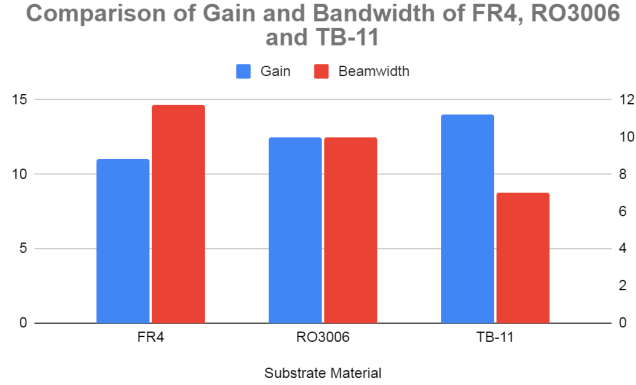


Figure 4.15: Comparison of Gain and Beamwidth of antenna array

Coordinatograph method, where the creation of the mask for the appropriate antenna shape is accomplished through the use of a coordinate graph. [72]. When the dimension of any section of the antenna is less than 100 micrometers, a semi-automatic photoplotter is employed to create the masks for the antenna. The semi-automatic photoplotter is capable of working with resolutions of up to 40 micrometers. The mask is an exact duplicate of the antenna geometry that is required. Afterward, the antenna is constructed on the substrate using the appropriate materials. The fabrication process of the research is carried out and conducted at Gandhinagar.

Figure 4.16 and 4.17 are the photographs of the final array antenna.

4.7 Testing of the SLTL-TB11 Antenna Array

It is important to test the final array antenna that has been developed to assess the S11 parameter. This is accomplished through the use of the Vector Network Analyzer. This is used to test the antenna's performance. A network analyzer is a highly sophisticated and advanced piece of equipment that is mainly used to give the variation of S11 parameter versus frequency. It is used to characterize or measure the response of devices or antennas across the entire spectrum of radio frequency frequencies [73]. It is possible to characterize the device or antenna by measuring its response, and from this information, it is possible to determine whether or not



Figure 4.16: Fabricated Image of Antenna array along with Researcher



Figure 4.17: A close image of the fabricated SLTL-TB11 array antenna

the equipment is functioning as planned.

The gain of array antenna is evaluated in an anechoic chamber, which preserves the perfect circumstances for evaluating an antenna during the testing process. It is possible to create an anechoic chamber by applying radio-wave absorbing material

to the walls, ceiling, and floor of a shielded room. Chambers can be as small as a tabletop enclosure, but they are typically larger than a room and large enough for engineers to walk in and work. This set was conducted at Sahajanand Laser Technology, Gandhinagar.

4.8 Validation of the simulated result with measured results

The proposed design is simulated in CST software. The S11 parameter is recorded as a function of frequency in X band of operation. The variation of the S11 parameter of the proposed design antenna using SLTL substrate is illustrated in Figure 4.18. It is observed that the design resonates at precisely 10 GHz, with an impedance bandwidth of 110 MHz. The S11 parameter of the proposed antenna array is -19 dB with simulation and -17 dB with measurement. The close proximity of the two readings gives good validation of the results.

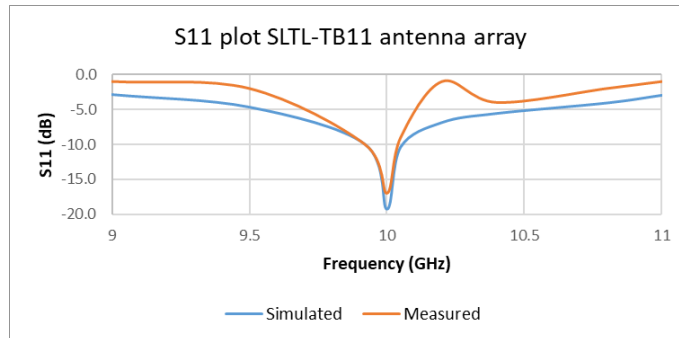


Figure 4.18: Validation of S11 parameter of antenna array using SLTL-TB11

The variation of gain is recorded for the frequency ranging from 9 GHz to 11 GHz for the proposed SLTL antenna array. The variation of gain for both the simulation and measurement works is illustrated in Figure 4.19, which shows a comparison between simulation and measurement work. The simulated antenna shows a gain of 14 dB at the resonance frequency of 10 GHz, and the measured gain is 12 dB at the same frequency. The measurement results follow the simulated results which validate

our design. A high measured gain of 12 dB justifies its usage in the imaging purpose.

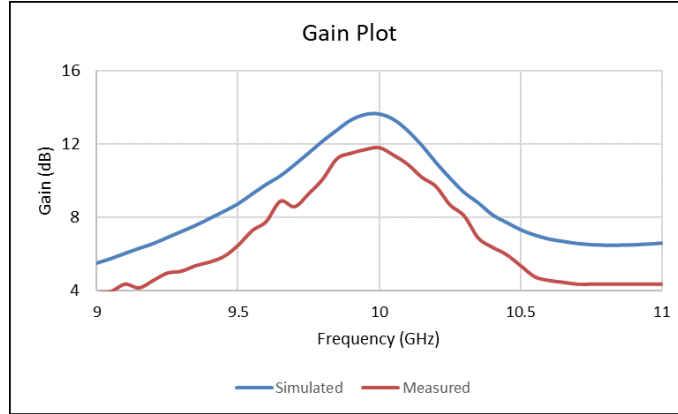


Figure 4.19: Validation of Gain of antenna array using SLTL-TB11

Table 4.5 below shows the simulated and measured results.

Parameter	Simulated	Measured
S11	-19.3 dB	-17.4 dB
Gain	-14 dB	-12 dB

Table 4.5: Result of the simulated and measured work of Antenna array using SLTL-TB11 substrate

4.9 Chapter Summary

Three microstrip array antenna designs with three different substrates namely FR4, RO3006 and self designed STBL, have been explored in this chapter. All the three proposed antenna designs were simulated using CST software. By comparing the simulated outcomes of all three proposed designs, it has been discovered that the microstrip antenna with STBL substrate outperforms the other two antennas and is suited for coastal security applications. Furthermore, the final designed array antenna using STBL is validated by testing its parameters in VNA and anechoic

chamber. The validation results confirms its superiority (high gain, low beamwidth and mechanical flexibility) and finds its suitable for the coastal surveillance.

Chapter 5

Coastal Surveillance Application of the Proposed Antenna Arrays

In this chapter the Intrusion Detection over a wide coastal line is tested using the developed Antenna Arrays on a Laboratory Setup as well as the live coastal region. The foundation of implementation methodology is laid on the Microwave Detection mechanism where Microwave beams are used in the sensor technology, where a transmit antenna generates the beams to form a spot on the receiver. If the receiver detects a difference in the received power, the system immediately begins to analyse the intrusion possibilities and, if the predetermined conditions for an incursion are met, an alarm is sounded to alert the control room. The system is capable of working even in non-favourable weather conditions. The designed Microwave imaging system is based on Microwave Object Detection Algorithms that will be able to detect human and other ‘intrusive’ objects without human intervention [74]. The sensor node will efficiently send the sensor data to the hub through wireless link. The prototype model is set up in the simulated lab to address the detection of intrusion sensing, alarm communication and assessment. The algorithm based on correlation method is employed for intrusion detection in long, flat, narrow geometrical zones/border areas. The entire system was implemented and tested at Laboratory in a simulated environment as well as live on the river site in Ahmedabad. As a result the data obtained from the simulated laboratory environment and river site were deeply anal-

ysed through ‘Digital Signal Processing Techniques’ [75]. The outcomes obtained are encouraging, where human and non-human intrusions were detected, after ‘Digital Signal Processing’ with an existing ‘Edge Gateway Electronic System’ located near the receiver antenna at the coastal site [76].

5.1 Test setup and Data collection

The pair of patch antenna arrays are designated as transmit and receive sensors based on their functionality.

Figure 5.1 illustrates the Lab setup for capturing the experimental data. The input signal (0 dB) of 10 GHz is fed to the RF amplifier. The transmitting gain is set to 20 dB. The RF amplifier power is fed to the transmit antenna.

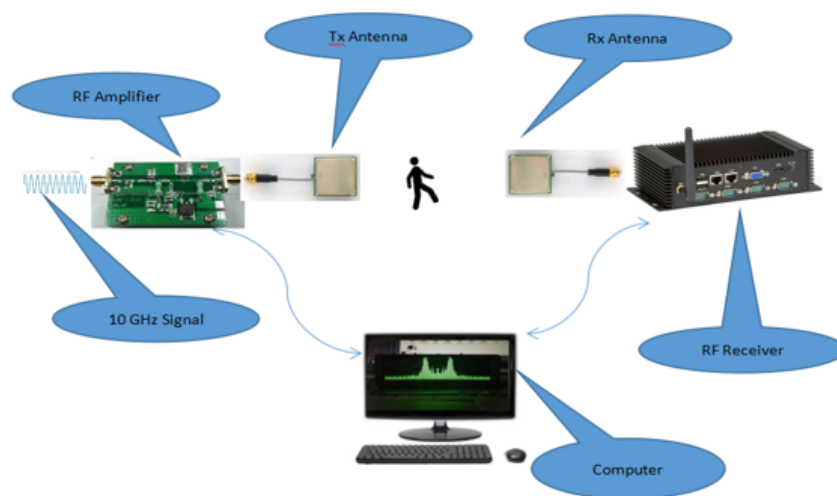


Figure 5.1: Schematic block of Test setup to capture intruder data

On the receiver side, a RF receiver is connected to the receiving antenna. The computer is connected to an RF receiver to collect the signal of the receiving antenna. The data was captured at every step of the intrusion and were recorded on the computer.

The detailed functioning of receiver and transmitter are illustrated in terms of block diagram as shown in Figure 5.2 and Figure 5.3 respectively.

As an intruder moves from top to bottom at different distances from Tx-antenna, the power drop pattern changes as tabulated in Table 5.1. The scale of the model is scalable by controlling the transmit power for desired distance from 1 to 10 kilometers. The developed patch antenna framework is designed to work under the scale factor of 1:100 under the Lab framework.

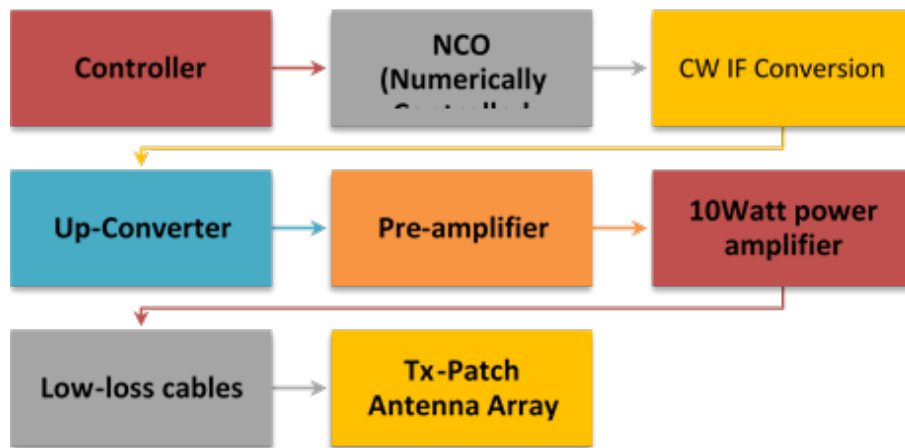


Figure 5.2: Block diagram illustrating the functioning of Transmitter

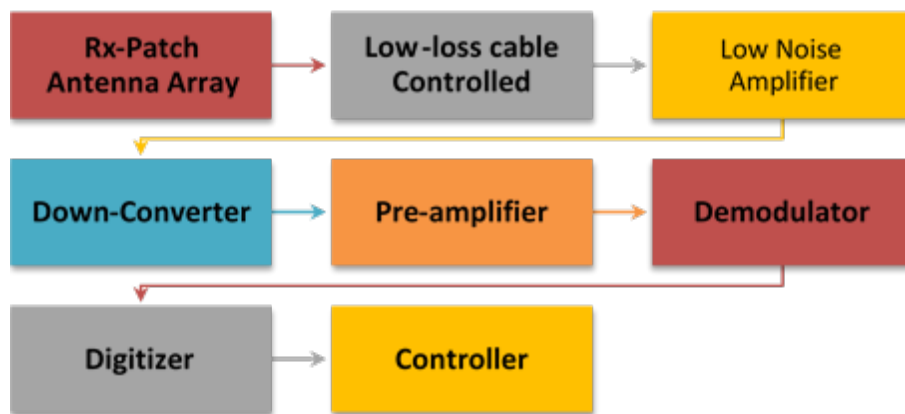


Figure 5.3: Block diagram illustrating the functioning of Receiver

Table-5.1 shows the statistics of the received power based on the intruder entering tangential to the ‘beam’ and the distance from Tx sensor.

5.2 Gain and Distance Calculations

Antenna gain is closely related to the directivity, but it is also a measure that takes into account the efficiency of the antenna. The gain of an antenna in a given direction is defined as the ratio of the intensity, in a given direction, and the radiation intensity that would be obtained if the power accepted by the antenna were radiated isotropically. This is called the absolute gain. The radiation intensity corresponding to the isotropically radiated power is equal to the power input by the antenna divided by 4π . Thus,

$$G(\phi, \theta) = 4\pi U(\phi, \theta) \cdot P_{in} \quad (5.1)$$

where P_{in} is the total input power. In addition, the total radiated power P_{rad} is related to the total input power P_{in} . Hence, it follows that

$$P_{rad} = e \cdot P_{in} \quad (5.2)$$

where, e is the antenna radiation efficiency defined as the ratio of the power delivered to the radiation resistance R_r and radiation losses R_L

$$e = R_r / (R_r + R_L). \quad (5.3)$$

Radiation efficiency can be considered as a measure of the dissipative or heat losses in an antenna. It is worth noting that impedance mismatch losses at the input port of the antenna are not included in the radiation efficiency.

For calculating the scalability of the model used in the Lab, the following equation, which will calculate the Free Space Path Loss at given frequency [77].

$$FSPL = 20\log_{10}(d) + 20\log_{10}(f) + 20\log_{10}\left(\frac{4\pi}{c}\right) - G(T_x) - G(R_x). \quad (5.4)$$

here, d = Distance between the antennas.

f = Frequency.

$G(\text{Tx})$ = The Gain of the Transmitting Antenna.

$G(\text{Rx})$ = The Gain of the Receiving Antenna.

c = Speed of light in vacuum.

In lab conditions:

$d = 1$ meter, $f = 10$ GHz, $G(\text{Tx}) = 14$, $G(\text{Rx}) = 14$.

Transmitter amplifier gain = 1, Receiver amplifier gain = 25.

Free space path loss become to around 27 dB.

Calculations for actual site conditions:

$d = 10$ kilometer, $f = 10$ GHz, $G(\text{Tx}) = 14$, $G(\text{Rx}) = 14$.

Transmitter amplifier gain = 2, Receiver amplifier gain = 60.

Free space path loss become to around 71 dB.

The distance between transmitting and receiving antennae of 10 kilometers are comfortably detectable with the sensitivity of the receiver of -60 dBm. The distance can be increased 25 kilometers by increasing the sensitivity of the Rx-receiver by 10 more dB.

To eliminate the noise and interferences, the received signal was sampled at 100 times in the second and was averaged on 100 datasets. So, one sample is connected at every second. The noise and interference is further reduced by applying 6th order polynomials [78].

$$p_{poly} = \sum_{m=0}^k a_{m+1} l^{k-m}, \quad k = 6 \quad (5.5)$$

Using above polynomial, the detection ability increases and falls alarms get reduced significantly. By considering the received signal as a Gaussian image, the following efforts are made.

To remove static background, multiple backgrounds have been generated. One will

be a master background, which will be derived from several backgrounds under different light and tide conditions. Besides, floating vegetation, leaves, etc has been removed to detect the target efficiently [79].

Object based classification describes the image processing through ‘objects’ and ‘vectors’ [80]. This reduces the processing time to a great extent. On the other hand, knowledge based Algorithms talk about linking low level image features with high level visual semantics. This provides a great amount of ‘automation’ capabilities to visualize the objects [81].

Source Inversion method using a multiplicative weighted L2-norm, total variation regularization is applied [82]. The location and contour shape are determined using two different reconstruction algorithms, a Newton-Kantorovich (NK) method and the modified gradient (MG) method whose effectiveness and robustness are compared. Both methods are based on domain integral representations of the field in the body [83].

Through the experiments, it is found that the received power fluctuates within 1 to 2 dB. If human or human sized objects intrude between the transmit and receive sensors, the power received on the receive sensor falls down by 7 to 10dB than nominal power received at the receiving sensor under “no intrusion” conditions. . Based on the geographical and environmental conditions of the site, the “Alert threshold” is set between 3 to 5dB. Drop in received power is the function of the object size and the distance from the transmitting sensor.

5.3 Results and Discussion

Under the research the target parameters of power drop 20 to 22 dB, distance of 8 to 10 kilometers. Through the adopted methodology, the target achieved as 19 to 22 dB attenuation with human intrusion, and 10 kilometr and with enhanced parameters of Rx-receiver, it can be achieved as high as 25 kilometers.

The reasons for the difference are environmental conditions, inaccuracies in sensor fabrications and instrument errors.

The excellent data were received in the Lab condition which are tabulated in Table-5.1.

5.3.1 Safety considerations

Considering safety against the high power RF radiations, the transmitter power is kept at safe level of less than 10dBm [84].

Radiation efficiency can be considered as a measure of the dissipative or heat losses in an antenna. It is worth noting that impedance mismatch losses at the input port of the antenna are not included in the radiation efficiency.

5.4 Summary of chapter

This chapter provides the details of the end application of the customized patch antenna arrays fabricated using highly customized dielectric material.

The effect of the intruder is tabulated, which numerifies as the drop of the received power as function of the size and speed of the intruder.

Step No.	Distance from transmitting sensor (m)									Remarks
	1 m	3 m	5 m	7 m	9 m	11 m	13 m	15 m	17 m	
Step 1	1.3	1.2	1.1	1	0.9	0.75	0.5	0.3	0.15	Drop in power
Step 2	1.4	1.3	1.2	1.1	1	0.9	0.5	0.3	0.15	
Step 3	1.5	1.4	1.3	1.2	1.1	1	0.75	0.55	0.4	
Step 4	1.6	1.5	1.4	1.3	1.2	1.1	0.85	0.62	0.46	
Step 5	1.7	1.6	1.5	1.4	1.3	1.2	0.95	0.75	0.55	
Step 6	1.9	1.8	1.7	1.69	1.63	1.23	1.09	1.04	0.8	
Step 7	2.8	2.5	2.43	2.05	2.01	1.98	1.87	1.54	1.38	
Step 8	3.6	3.45	3.37	3.2	3.08	2.5	2.03	1.6	1.4	
Step 9	5.58	5.15	4.72	4.05	3.7	2.8	2.23	2.03	1.9	
Step 10	11.66	11.2	10.74	9.8	8.9	8.44	7.96	7.5	7.04	
Step 11	16.32	15.9	15.45	14.93	13.8	13.38	12.96	12.5	12.08	
Step 12	22.1	21.1	20.11	19.11	18.11	17.11	17.62	17.14	16.66	
Step 13	22.5	21.5	20.5	19.4	18.4	17.4	20.42	19.92	19.44	Intruder in center
Step 14	22	21.2	20.21	19.21	18.21	17.96	17.54	17.11	16.69	
Step 15	15.94	15.5	15.05	14.3	13.3	12.86	12.42	11.98	11.54	
Step 16	10.3	9.9	9.5	8.89	7.9	7.5	7.1	6.7	6.3	
Step 17	4.88	4.5	4.12	3.46	2.87	2.66	2.28	1.87	1.49	
Step 18	3.7	3.56	3.43	3.21	2.63	2.39	2.16	1.76	1.34	
Step 19	2.9	2.76	2.64	2.57	2.38	2.27	2.05	1.63	1.21	
Step 20	1.8	1.68	1.53	1.42	1.35	1.26	1.17	1.04	0.85	

Table 5.1: Drop in Received Power Level (in dB) against the movement of intruder

Chapter 6

Conclusion and Future Work

The formulated problem in research work was based on the theme of “National Security in monitoring intrusion detection on coastal regions of India”.

6.1 Conclusion

In this work new substrate material is synthesized with superior dielectric, thermal and mechanical performance over its marketing competitors, FR4 and RO3006. The new substrate given the name SLTL-TB-11 and used to designed the microstrip patch antenna array as a receiver and transmitter sensors. To realize this sensor, microstrip patch antenna was simulated, fabricated and characterized. The performance (gain and beamwidth) of the proposed antenna was evaluated by comparing with antennas designed and simulated with FR4 and RO3006 substrate. Finally, the Intrusion Detection over a wide coastal line was tested using the developed Antenna Arrays on a Laboratory Setup as well as the live coastal region. The outcomes obtained are encouraging, where human and non-human intrusions were detected, after ‘Digital Signal Processing’ with an existing ‘Edge Gateway Electronic System’ located near the receiver antenna at the coastal site.

The following observations have been made:

- The dielectric constant of 10.5 was realized which help us to reduce the size and weight of the antenna sensors.
- The loss tangent 0.0016 was achieved. The low loss tangent led the higher gain and low thermal losses inside the antenna.
- The thermal Coefficient was brought as low as 15 ppm/°C . This reduction brings much higher temperature stability of the antenna.
- The dimensional stability played a major role in the fabrication process of ‘multi-patch’ antennas. The achieved values from 2.7 to 0.2 mm/m makes the fabrication process simpler and awards long-term reliability.
- Tensile modulus plates play a very critical role in maintaining the flexibility of the antenna for long term stability against bending in, mechanical stresses, and vibrations. We were successful in achieving 189 Kpsi dimensional stability for stable operation and longer serving life of the antenna.
- Moisture absorption is one of the most critical parameters for maintaining stable dielectric values for consistency performance of the antenna against changing moisture across the year; especially on the coastal line. We were successful in achieving as low as 0.017% moisture absorbance.
- With TB-11 substrate, resonant frequency of 10 GHz, return loss, of -19.3 dB, VSWR of 1.24, of 14 dB, beamwidth of 7 degree were achieved.
- Under the research the target parameters of power drop 20 to 22 dB, distance of 8 to 10 kilometers.
- The pair of patch antenna arrays were designated as transmit and receive sensors based on their functionality. The developed patch antennas are to be used in a setup framework to be installed at the coastal line - the actual site.
- Very encouraging results were achieved in the Lab testing of TB-11 based patch array antenna. A significant drop of about 18dB was observed with human and human size intruders. The Lab model is scalable for actual coastal

line conditions by just changing the distance between transmit and receive antenna and increasing the pulse power of the transmit antenna.

- Through the adopted methodology, the target achieved as 19 to 22 dB attenuation with human intrusion, and 10 Km range and with enhanced parameters of Rx-receiver, it can be achieved as high as 25 kilometers.
- The sensors are very power efficient, which can work with about 1sq feet of solar panel for a week even if it has a chance to charge once a week only.

6.2 Future Scope

During the Research and Experimentation, many interesting observations were noticed, which encouraged future work.

- Human and Non-human intruders reflect and refract a detectable amount of Microwave x-band frequencies. These features add a few more dimensions to improvise the Intrusion detection and other security use cases.
- K and KA Band gives quite good absorptions and scattering due to water and more to salty water. This phenomenon can help to sense intrusion on icy mountains and valleys.
- 3D Patch Antenna can be a sturdy and efficient sensor for Intrusion detection of the span of 10 kilometers or so.
- A very compact and Micro Radar sensor can be built for automotive safety purposes also.

The Microwave Imaging can be optimized for many more use cases. Microwave imaging approach enhances to detect and identify unknown objects and security threat level detection as well.

Multi-beam topology can further enhance the functionality of a doppler effect similar to “Microwave RADAR” as a micro-RADAR for automotive applications.

Bibliography

Bibliography

- [1] Kraus, J.D. (1985), Antenna since Hertz and Marconi, IEEE Transaction on Antenna and Propagation, Vol. 33, No. 2, pp. 131-137.
- [2] Balanis, C.A. (1992), Antenna Theory: A review, Proceeding of IEEE, Vol. 80, No. 1, pp. 7-23.
- [3] Collin, R.E. (1985), Antenna and Radio-wave Propagation, McGraw Hill.
- [4] Deschamps, G. A.(1953), Microstrip Microwave Antennas, Third Symposium on the USAF Antenna Research and Development Program, University of Illinois, Monticello, Illinois, October 18-22.
- [5] Munson, R. E. (1972), Microstrip Phased Array Antenna, 22nd Annual USAF Antenna Symposium.
- [6] Bahal, I.J., and Bhatia, P. (1980) Microstrip antenna. Artech House, New York.
- [7] James, J. R., Hall, P. S., and Henderson, A. (1981), Some Recent Development in Microstrip Antenna Design, IEEE Transaction on Antennas and Propagation, Vol. 29, pp. 124-128.
- [8] Mailloux, R. J., McIlvanna, J.F. and Kernweis, N. P. (1981), Microstrip Array Technology, IEEE Transaction on Antennas and Propagation, Vol. 29, pp. 25-37.
- [9] Ranjan Mishra, (2016), An Overview of Microstrip Antenna, HCTL Open International Journal of Technology Innovations and Research (IJTIR), Vol 21, Issue 2, pp 1-17.
- [10] Lee, H. F., and Chen, W. (1997), Advances in Microstrip and Printed Antennas, John Wiley & Sons, New York.

- [11] Ammann M.J. and Chen, Z.N. (2003), Wideband monopole antennas for multi-band wireless systems, *IEEE Antennas and Propagation Magazine*, vol. 45, pp. 146-150.
- [12] Guha, D., and Antar Yahia, M. M. (2011), *Microstrip and Printed Antennas: New Trends, Techniques and Applications*, John Wiley & Sons, New York.
- [13] Herscovici, N. (1998), A Wideband Single Layer Patch Antenna, *IEEE Transaction on Antennas and Propagation*, vol. 46, pp. 471-473.
- [14] Kapil Saraswat and Ayyangar R. Harish. (2018), Dual-band CP coplanar waveguide-fed split-ring resonator-loaded G-shaped slot antenna with wide-frequency ratio. *IET Microwaves, Antennas Propagation*, Vol. 12, pp. 1920-1925.
- [15] K. Kandasamy, B. Majumder, J. Mukherjee and K. P. Ray. (2016), Dual-Band Circularly Polarized Split Ring Resonators Loaded Square Slot Antenna” *IEEE Transactions on Antennas and Propagation*, Vol. 64, No 8, pp 1-6.
- [16] Taiwei Yue, Zhi Hao Jiang, Anastasios H. Panaretos and Douglas. H. Werner (2017), A Compact Dual-band Antenna Enabled by a Complementary Split Ring Resonator Loaded Metasurface, *IEEE transaction on Antenna Propagation*.
- [17] F. Farzami, K. Forooghi, and M. Norooziarab (2011), Miniaturization of a Microstrip Antenna Using a Compact and Thin Magneto-Dielectric Substrate, *IEEE Antennas And Wireless Propagation Letters*, Vol 10, pp. 1540-1542.
- [18] Hassan Mirzaei, and George V. Eleftheriades. (2011), A Compact Frequency-Reconfigurable Metamaterial-Inspired Antenna. *IEEE Antennas and Wireless Propagation Letters*, Vol 10. 10, pp. 1154-1157.
- [19] C. d. F. L. de Vasconcelos, M. R. M. L. de Albuquerque, S. G. da Silva, J. d. R. S. Oliveira and A. G. d’Assunção, (2011), Full-Wave Analysis of Annular Ring Microstrip Antenna on Metamaterial, *IEEE Transactions on Magnetics*, Vol. 47, no. 5, pp. 1110-1113.
- [20] Dongying Li, Zsolt Szabó, Xianming Qing, Er-Ping Li, and Zhi Ning Chen, (2012), A High Gain Antenna With an Optimized Metamaterial Inspired Super-

- strate" IEEE Transactions on Antennas and Propagation, Vol. 60, No. 12, pp. 6018-6023.
- [21] M. S. Majedi and A. R. Attari, (2013), A Compact and Broadband Metamaterial Inspired Antenna. IEEE Antennas and Wireless Propagation Letters, Vol. 12, pp. 345-348.
- [22] Seung-Tae Ko and Jeong-Hae Lee , (2013), Hybrid Zeroth-Order Resonance Patch Antenna With Broad E-Plane Beamwidth. IEEE Transactions on Antennas and Propagation, Vol. 61, No. 1, pp.19-25.
- [23] Li-Ming Si, Weiren Zhu, and Hou-Jun Sun. (2013), A Compact, Planar, and CPW-Fed Metamaterial-Inspired Dual-Band Antenna. IEEE Antennas and Wireless Propagation Letters, Vol. 12, pp. 305-308.
- [24] R. Mishra, R.G. Mishra, R.K. Chaurasia, A.K. Shrivastava, (2019) Design and Analysis of Microstrip Patch Antenna for Wireless Communication, International Journal of Innovative Technology and Exploring Engineering, Vol-8 Issue-7, pp 663-666.
- [25] R. Rashmitha, N. Niran, A, Abhinandan, M. R. Ahmed, (2020) Microstrip Patch Antenna Design for Fixed Mobile and Satellite 5G Communications, Procedia Computer Science, Volume 171, Pages 2073-2079.
- [26] K.Leela Rani, P.Siddaiah, 1×4 Rectangular Patch Array Operating at 10 GHz Using Corporate Feeding Technique, International Journal of Engineering Development and Research, Volume 5, Issue 2, pp 845-848.
- [27] Mohamed Aly Aboul-Dahab, Hussein Hamed Mahmoud Ghouz, Ahmed Zakaria Ahmed Zaki, (2016) High Gain Compact Microstrip Patch Antenna for X-Band Applications, International Journal of Antennas and Propagation, Vol.2, No.1, pp 47-58
- [28] Kumaresh Sarmah, Angana Sarma, Kandarpa Kumar Sarma, Sunandan Baruah, (2015) Dual-Band Microstrip Patch Antenna Loaded with Complementary Split Ring Resonator for WLAN Applications, , Advances in Intelligent Systems and Computing, Vol 339. pp 573-580

- [29] Farhad Farzami, Keyvan forooraghi, and Majid Norooziarab, (2012) Miniaturization of a microstrip antenna using a compact and thin magneto-dielectric substrate, *IEEE Transactions on Antennas and Propagation*, Vol 54, no 11, pp 3391 – 3399.
- [30] H.Mirzaei,G.Eleftheriades, (2011) A Compact Frequency-Reconfigurable Metamaterial-Inspired Antenna, *IEEE Antennas and Wireless Propagation Letters* , Vol 10, pp 1154-1157.
- [31] M. S. Majedi; A. R. Attari (2013) Compact and Broadband Metamaterial-Inspired Antenna, *IEEE Antennas and Wireless Propagation Letters*, Volume 12, pp 345-348.
- [32] P. Mookiah,and K.R. Dandekar, (2009), Metamaterial-Substrate Antenna Array for MIMO Communication System, *IEEE Transactions on Antennas and Propagation*, Vol. 57. No 10, pp. 3283-3292.
- [33] Seung-Tae Ko; Jeong-Hae Lee (2013) Hybrid Zeroth-Order Resonance Patch Antenna With Broad E-Plane Beamwidth, , *IEEE Transactions on Antennas and Propagation* Volume: 61, Issue: 1, pp 19-25.
- [34] R.Islam and G.V. Eleftheriades, (2010), On the Independence of the Excitation of Complex Modes in Isotropic Structures” *IEEE Transactions on Antennas and Propagation*, Vol. 58, No. 5, pp.1567-1578.
- [35] Pai Yen Chen, and Andrea Alu, (2010), Sub-Wavelength Elliptical Patch Antenna Loaded With μ -Negative Metamaterials” *IEEE Transactions on Antennas and Propagation*, Vol. 58, No. 9, pp.2909-2919.
- [36] Li-Ming Si, Weiren Zhu, Hou-Jun Sun, (2013) A Compact, Planar, and CPW-Fed Metamaterial-Inspired Dual-Band Antenna, *IEEE Antennas and Wireless Propagation Letters* , Vol. 12, pp. 305-308.
- [37] Mahmoud A. Abdalla and Ahmed Fouad, (2016) Integrated Filtering Antenna Based on D-CRLH Transmission Lines for Ultra-Compact Wireless Applications, *Progress In Electromagnetics Research C*, Vol. 66, pp 29–38.

- [38] Hussein Attia, Leila Yousefi, and Omar M. Ramahi, (2011), Analytical Model for Calculating the Radiation Field of Microstrip Antennas With Artificial Magnetic Superstrates: Theory and Experiment" IEEE Transactions on Antennas and Propagation, Vol. 59, No. 5, pp.1438-1445.
- [39] M.M. Islam, M.T. Islam, (2015) Compact metamaterial antenna for UWB applications, Electronics Letters, Volume 51, Issue 16 p. 1222-1224.
- [40] John L. Volakis, and Kubilay Sertel, (2011), Narrowband and Wideband Metamaterial Antennas Based on Degenerate Band Edge and Magnetic Photonic Crystals, Proceedings of the IEEE, Vol. 99, No. 10, pp. 1732-1745.
- [41] N. Singh, S. Singh and H. Kumar, (2011), A study on Applications of Metamaterial based Antennas, 3rd IEEE International Conference on Electronics Computer Technology, pp. 192-196.
- [42] G. Jang and S. Kahng, (2011), Compact metamaterial zeroth-order resonator bandpass filter for a UHF band and its stopband improvement by transmission zeros, IET Microwave Antennas / Propagation, Vol. 5, Issue. 10, pp. 1175–1181.
- [43] H. Attia, O. Siddiqui and O. M. Ramahi, (2011), Analysis of gain enhancement in antenna arrays covered with metamaterial superstrates using transmission line modeling, IEEE International Symposium on Antennas and Propagation (APSURSI), pp. 557-560.
- [44] H. Mirzaei and G. V. Eleftheriades, (2011), A wideband metamaterial-inspired compact antenna using embedded non-Foster matching," IEEE International Symposium on Antennas and Propagation (APSURSI), pp. 1950-1953.
- [45] Haider R. Khaleel, Hussain M. Al-Rizzo, Daniel G. Rucker, Yasir A. Rahmatallah, and Seshadri Mohan "Mutual Coupling Reduction of Dual-band Printed Monopoles Using MNG Metamaterial" IEEE, pp.2219-2222, 2011.
- [46] Youn-Kwon Jung and Bomson Lee, (2012), Dual-Band Circularly Polarized Microstrip RFID Reader Antenna Using Metamaterial Branch-Line Coupler, IEEE Transactions on Antennas and Propagation, Vol. 60, No. 2, pp.786-791.

- [47] Yuandan Dong, Hiroshi Toyaoand Tatsuo Itoh, (2012), Design and Characterization of Miniaturized Patch Antennas Loaded With Complementary Split-Ring Resonators, *IEEE Transactions on Antennas and Propagation*, Vol. 60, No. 2, pp.772-785.
- [48] Ming-Chun Tang, Shaoqiu Xiao, Bingzhong Wang, Jian Guan, and Tianwei Deng, (2011), Improved Performance of a Microstrip Phased Array Using Broad band and Ultra-Low-Loss Meta material Slabs, *IEEE Antennas and Propagation Magazine*, Vol. 53, No. 6, pp.31-41.
- [49] Raoul O. Ouedraogo, Edward J. Rothwell, Alejandro R. Diaz, Kazuko Fuchi, and Andrew Temme, (2012), Miniaturization of Patch Antennas Using a Metamaterial-Inspired Technique, *IEEE Transactions on Antennas and Propagation*, Vol. 60, NO. 5, pp. 2175-2182.
- [50] Xin Mi Yang, Xue Guan Liu, Xiao Yang Zhou, and Tie Jun Cui, (2012), Reduction of Mutual Coupling Between Closely Packed Patch Antennas Using Waveguided Metamaterials, *IEEE Antennas and Wireless Propagation Letters*, Vol. 11, pp. 389-391.
- [51] Bimal Garg, Nitin Agrawal, Vijay Sharma, Ankita Tomar and Prashant Dubey, (2012), Rectangular Microstrip Patch Antenna with “Pentagonal Rings” Shaped Metamaterial Cover, *International Conference on Communication Systems and Network Technologies*, pp. 40-44.
- [52] Zhenzhe Liu, Peng Wang, and Zhiyi Zeng, (2013), Enhancement of the Gain for Microstrip Antennas Using Negative Permeability Metamaterial on Low Temperature Co-Fired Ceramic (LTCC) Substrate, *IEEE Antennas and Wireless Propagation Letters*, Vol. 12, pp.429-432.
- [53] Seyed Mohammad Hashemi, Mohammad Soleimani and Sergei A. Tretyakov, (2013), Compact negative-epsilon stop-band structures based on double-layer chiral inclusions, *IET Microwave Antennas Propagation* , Vol. 7, No 8, pp. 621–629.
- [54] Falguni Raval, Dr Y P Kosta, Jagruti Makwana and Amit V Patel, (2013), Design Implementation of Reduced size Microstrip Patch Antenna with Meta-

material Defected Ground Plane, International conference on Communication and Signal Processing, pp.186-190.

- [55] Mahmoud A. Abdalla and Ahmed Fouad, (2016), "Integrated Filtering Antenna Based on D-CRLH Transmission Lines for Ultra-Compact Wireless Applications" Progress In Electromagnetics Research C, Vol. 66, pp. 29– 38.
- [56] Mahmoud A. Abdalla, Ahmed A. Ibrahim, and Mohammed H. Abd El-Azeem, (2015), "Phase Enhancement for Multi-Resonance Compact Metamaterial Antennas," Progress In Electromagnetics Research C, Vol. 60, pp.83–93.
- [57] Wenquan Cao, Zuping Qian, Bangning Zhang and Zhi Ning Chen, (2014), "Applications of Metamaterials-Based Microstrip Antennas," 3rd Asia-Pacific Conference on Antennas and Propagation, pp.77-80.
- [58] M.M. Islam, M.T. Islam, M. Samsuzzaman and M.R.I. Faruque, (2015), "Compact metamaterial antenna for UWB Applications," Electronics Letters Vol. 51 No. 16 pp. 1222–1224.
- [59] Gaurav K. Pandey, Hari S. Singh, Pradutt K. Bharti, and Manoj K. Meshram, (2014), "Metamaterial Based Compact Antenna Design for UWB Applications," IEEE Region 10 Symposium, pp. 15-18.
- [60] R. Seviour, Y.S. Tan and A. Hopper , (2014), "Effects of High Power on Microwave Metamaterials," 8th International Congress on Advanced Electromagnetic Materials in Microwaves and Optics - Metamaterials 2014, Copenhagen, Denmark, pp.142-144.
- [61] Bhardwaj, D., Soni, B., Bhatnagar, D., and Sancheti, S. (2008). "Design of square patch antenna with a notch on FR4 substrate." IET Microwaves, Antennas & Propagation, 2(8), 880–885
- [62] Coombs C.,(2001) "Printed circuit handbook", McGraw Hill, fifth edition.
- [63] <https://www.ccieurodam.com/en/products/rogers-rf-microwave-materials>.
- [64] AL-Oqla, F. M., & Omar, A. A. (2014). "An expert-based model for selecting the most suitable substrate material type for antenna circuits." International Journal of Electronics, 102(6),

- [65] D. Thomas, J. Chameswary and M. T. Sebastian, (2009) Dielectric properties of butyl rubber-SrTiO₃ flexible composite, 2009 Applied Electromagnetics Conference (AEMC), pp. 1-3.
- [66] Sabisky, E. S., Gerritsen, H. J. (1962). Measurements of Dielectric Constant of Rutile (TiO₂) at Microwave Frequencies between 4.2° and 300°K. *Journal of Applied Physics*, 33(4), pp. 1450–1453.
- [67] Sylvain Marinel, Doo Hyun Choi, Romain Heuguet, Dinesh Agrawal, Michael Lanagan, (2013). Broadband dielectric characterization of TiO₂ ceramics sintered through microwave and conventional processes, *Ceramics International*, Vol 39, Issue 1, pp 299-306.
- [68] Hakim, I. K., Bishai, A. M., Saad, A. L. (1988). Dielectric properties of butyl rubber mixtures at 1061010 Hz. *Journal of Applied Polymer Science*, 35(4), pp 1123–1125.
- [69] Thomas, D., Janardhanan, C., Sebastian, M. T. (2011). Mechanically Flexible Butyl Rubber-SrTiO₃ Composite Dielectrics for Microwave Applications. *International Journal of Applied Ceramic Technology*, 8(5), pp. 1099–1107.
- [70] Janardhanan, C., Thomas, D., Subodh, G., Harshan, S., Philip, J., and Sebastian, M. T. (2011). Microwave dielectric properties of flexible butyl rubber-strontium cerium titanate composites. *Journal of Applied Polymer Science*, 124(4), pp. 3426–3433. .
- [71] A. D. Vyas, V. A. Rana, D. H. Gadani and A. N. Prajapati,(2008) Cavity perturbation technique for complex permittivity measurement of dielectric materials at X-band microwave frequency, *International Conference on Recent Advances in Microwave Theory and Applications*, pp. 836-838,
- [72] Agafonov, K.V., Balyaev, B.A., and Leksikov, A.A. (2006), Automated Coordinatograph for Manufacture of Microstrip Circuits, 16th International Conference on Microwave and Telecommunication Technology, pp. 637-638.
- [73] Verspecht, J. (2005), Large Signal Network Analysis, *IEEE Microwave Magazine*, Vol. 6, No. 4, pp. 82-92.

- [74] Ata ur Rehman, Zeeshan Ellahi, Asif Iqbal, Farman Ullah, Ahmed Ali, Kyung Sup Kwak, (2019) "Design and Implementation of Directional Sensors for Privacy-Ensured Device-Free Target Localization in Indoor Environment", *Wireless Communications and Mobile Computing*, Vol. 2019, Article ID 8391307, 8 pages, 2019.
- [75] E. Ricci, S. Di Domenico, E. Cianca and T. Rossi, (2015) "Artifact removal algorithms for stroke detection using a multistatic MIST beamforming algorithm," 2015 37th Annual International Conference of the IEEE Engineering in Medicine and Biology Society (EMBC), pp. 1930-1933,
- [76] M. D. Perez et al., (2018) "New Approach for Clinical Data Analysis of Microwave Sensor Based Bone Healing Monitoring System in Craniosynostosis Treated Pediatric Patients," 2018 IEEE Conference on Antenna Measurements Applications (CAMA), pp. 1-4.
- [77] A. Al-Hourani, S. Kandeepan and A. Jamalipour, (2014) "Modeling air-to-ground path loss for low altitude platforms in urban environments," 2014 IEEE Global Communications Conference, pp. 2898-2904.
- [78] K Ravindra A D Sarma, M V S N Prasad, (2002) "An adaptive polynomial path loss model at UHF frequencies for mobile railway communication", *Indian Journal Radio and Space physics*, Vol. 31, pp, 278-284.
- [79] A. Zamani and A. M. Abbosh, (2015) "Fast multi-static technique for microwave brain imaging," *IEEE International Symposium on Antennas and Propagation USNC/URSI National Radio Science Meeting*, pp. 536-537.
- [80] Li, H., H. Gu, Y. Han, and J. Yang., (2010) "Object-oriented Classification of High-resolution Remote Sensing Imagery Based on an Improved Colour Structure Code and a Support Vector Machine." *International Journal of Remote Sensing* 31 (6), pp 1453–1470.
- [81] Shi Z. (2010) *Image Semantic Analysis and Understanding*. In: Shi Z., Vadera S., Aamodt A., Leake D. (eds) *Intelligent Information Processing V. IIP 2010*. IFIP Advances in Information and Communication Technology, Vol 340.

- [82] Van den Berg, P. M., Abubakar, A. (2001). Contrast Source Inversion Method: State of Art. Progress In Electromagnetics Research, 34, pp 189–218.
- [83] K. Belkebir, R. E. Kleinman and C. Pichot, (1997) "Microwave imaging- Location and shape reconstruction from multifrequency scattering data," in IEEE Transactions on Microwave Theory and Techniques, Vol. 45, no. 4, pp. 469-476.
- [84] D. D. Arumugam and a. D. W. Engels, (2008) "Impacts of RF radiation on the human body in a passive RFID environment," 2008 IEEE Antennas and Propagation Society International Symposium, pp. 1-4.

Publications

- [1] Madhukant Patel, Piyush Kuchhal, Kanhiya Lal, Ranjan Mishra, (2017) Design and Analysis of Microstrip Patch Antenna Array using Different Substrates for X-Band Applications, International Journal of Applied Engineering Research ISSN 0973-4562. Vol. 12, No 19. pp. 8577-8581 © Research India Publications. Scopus indexed

- [2] Madhukant Patel, Piyush Kuchhal, Kanhaiya Lal, Virendra Singh and Hemangi Patel, (2018) Design and Performance Analysis of High Gain Narrow Band Patch Antenna Arrays at X-Band, © Springer Nature Singapore Pvt Ltd. Intelligent Communication, Control and Devices, Advances in Intelligent Systems and Computing 624. Scopus indexed

- [3] Madhukant Patel, Veerendra Singh Jadaun, Kanhiya Lal, Piyush Kuchhal, (2018), Design of a High Gain Compact Circular Microstrip Patch Antenna for X-Band, International Journal of Engineering Technology, Vol.7, No 2, pp. 168-170. Scopus indexed

Scholar Resume

Madhukant Patel

B/202, Premier Apartment
Sandesh Press Road, Nr. Lad Society
Vastrapur, Ahmedabad – 380 054, India
Cell: (+91) 99250 27534.
email: madhukant.patel@reveautomation.com

Senior to top level positions in Research, Project Management, Product Development, Consulting with leading organizations and working with cutting edge technology

Overview

A seasoned professional with over 4.5 decades rich experience in Designing Electronics, Communications firmware based Product Development, Project Management, Strategy Planning, and Corporate training, Team Management with well known organisations in Electronics, Communication, Instrumentation, Automation, Robotics, etc.

Expertise in executing projects from Concept to Launch with focus on projects Scope and rendering end-to-end solutions. Possesses sound product knowledge and thorough understanding of design development of High-Reliability Systems for Industries, Broadcast, Defence Communications, and Industrial automation with abilities in optimising product performance and efficiencies.

An enterprising leader with abilities in leading multi-skilled motivated teams to achieving organisational goals and industry best practices. Have successfully worked on various projects. Design and realization of projects with ISRO, DRDO and other Govt. Organizations. Managed projects with MNCs with ISO9001 and CMMI processes.

The stints with leading organisations have honed abilities in identifying potential, deconstructing complex situations and further conceiving and implementing streamlined solutions that have led to increased revenues, profitability and overall success. Exceptionally well organised with a track record that demonstrates self motivation, creativity, and initiative to achieve both personal corporate goals.

Professional Qualification

- B.E. (Electronic Communications) from LD College of Engineering, Gujarat University, Ahmedabad, India with **1st Division** in 1983.
- M.E. (Electronics Communications) from DDIT, Gujarat University, India **1st Division** in 1992.
- Certificate course in Marketing Management from Indira Gandhi National Open University, New Delhi in 1995
- Diploma in Cene-projections (Part time) from Gujarat Technical board in 1996
- Registered as stater-up at IIC-PDPU, Gandhinagar for innovation of Smart soil sensors for Smart farming in 2018.

Research Experience at ISRO

Worked for more than 18 years in the field of Sensor Technology, Digital Signal Processing, and Image processing using Processors/ Controllers, CPLDs, FPGAs and High speed Analog and Digital Devices; High Tech. National and International Projects. Got inVolved in many challenging tasks like ‘System Integration’, ‘System reliability’, ‘Project Reviews’, etc.

MONEX (Monsoon Experiments in Arabian Sea) This was an international project to find out vertical weather profiles over the Indian Ocean. System was installed on board a ship and was tried out in the Arabian Sea for about one year. Actively participated in design/ development, installations of the on board ‘INS Vikrant’ and other Government research vessels. Experiments on board INS VIKRANT (Aircraft Carrier Warship of India) Gaveshnai (Research ship). Significantly installed and experimented an onboard system INS VIKRANT for gathering vertical wind profile over sea surface for ‘Guidance Parameter’ to Missiles. BioTech sensors, Data analytics, Quality assurance and quality control. Design of IoT based Wireless Sensors and sensor networks for Industrial, Smart cities, Home and Building Automation Hi-reliability designs with immunity against EMI-EMC, Embedded Designs, Corporate Training.

Domain Skill

Technical Advisor : During an Europe tour organised by FMC, supported by the World Bank and the Reserve Bank of India.

Research : BioTech sensors, Data analytics, Quality assurance and quality control Design of IoT based Wireless Sensors and sensor networks for Industrial,

Smart cities, Home and Building Automation Hi-reliability designs with immunity against EMI-EMC, Embedded Designs, Corporate Training.

IoT based design: CNC Machine monitoring systems, Textile engineering, and Pharma machineries.

Hardware and Software: Fortunate to work on a mission critical project where 99.99% reliability was to be proved. Have used Scientific algorithms, Analog and Digital Designs, VLSI/ CPLD and FPGA based designs, SoC (System on Chip) based System Designs, Signal Processing and so on.

Microcontroller and Microprocessors: Fortunate to work with several generations of Microprocessor and Microcontroller for vivid applications and for variety of domains like Space, Marine, Ground, Industrial, BioTech, Telecom, Agro-science, Biomedical, Entertainment, Education, Corporate training and many more.

Organisational Experience

- Since 2018 - Working as CTO, Teksun Microsys Private Limited.
- 2010 to 2018 - Established an IoT company named Reveautomation
- 2010 to 2012 - Chairman IETE (Gujrat)
- 2008 to 2010 - Chief Technical Officer at VisioSpect and JEKSONusa.
- 2006 to 2008 - Director–Engineering, Sahajanand Laser Technology Limited.
- 2004 to 2006 - Director–Engineering, e-Infochips Limited, Pune.
- 2000 to 2004 - General Manager, CG-CoreEl Logic Systems Ltd.
- 1996 to 2000 - Deputy General Manager, Syntel Telecom, Pune.
- **1977 to 1996** - Scientist/ Engineer, SAC/ ISRO, Ahmedabad.

Declaration

I vouch for the accuracy of the above-mentioned data. I pledge to put out my best efforts to meet high standards and contribute to India.

Madhukant Patel

MKP_thesis_19_Dec.pdf

ORIGINALITY REPORT

9%	8%	4%	%
SIMILARITY INDEX	INTERNET SOURCES	PUBLICATIONS	STUDENT PAPERS

PRIMARY SOURCES

1	ijtir.hctl.org Internet Source	4%
2	"Handbook of Antenna Technologies", Springer Science and Business Media LLC, 2016 Publication	1%
3	dokumen.pub Internet Source	1%
4	Madhukant Patel, Veerendra Singh Jadaun, Kanhya Lal, Piyush Kuchhal. "Design of a High Gain Compact Circular Microstrip Patch Antenna for X-Band", International Journal of Engineering & Technology, 2018 Publication	1%
5	dspace.library.iitb.ac.in Internet Source	1%
6	www.reveautomation.com Internet Source	1%
7	"Proceedings of the International Conference on Recent Cognizance in Wireless	1%

Communication & Image Processing", Springer Nature, 2016

Publication

8

www.tecnelco.com

Internet Source

1 %

9

hdl.handle.net

Internet Source

1 %

Exclude quotes Off

Exclude matches < 1%

Exclude bibliography On

Madhukant Patel